LARGE-SCALE BEACH CHANGE:

KAANAPALI, HAWAI'I

A THESIS SUBMITTED TO THE GRADUATE DIVISION OF THE UNIVERSITY OF HAWAII IN PARTIAL FULFILLMENT OF THE REQUIREMENTS FOR THE DEGREE OF

MASTER OF SCIENCE

IN

GEOLOGY AND GEOPHYSICS

DECEMBER 2002

By
Dolan Eversole

Thesis Committee:

Charles H. Fletcher, Chairperson
Mark Merrifield
Richard Grigg

ACKNOWLEDGMENTS

I would like to thank Charles Fletcher, who as the chair of my committee, encouraged me to push myself and explore further than I knew possible. I thank him for his technical support, guidance and friendship as an advisor, educator and mentor.
I thank the other members of my committee: Mark Merrifield and Richard Grigg for their generous time and effort spent helping me with this project. My committee has been instrumental in encouraging me to develop and explore new insights in my research, a process that has fostered new skills and wisdom for me to take with me through life

I would like to thank the faculty and staff of the Department of Geology and Geophysics at the University of Hawaii, Manoa for their support and technical expertise. I am especially grateful to the members of the Coastal Geology Group for their enthusiastic field support, suggestions, in-depth discussion and collaboration and friendship. I would like to acknowledge Kevin Bodge of Olsen Associates for his instrumental technical assistance in the practical application of longshore sediment transport models. I am also indebted to Jerome Aucan and Pat Caldwell of the Oceanography department for their technical assistance in retrieving and processing wave data. Technical assistance in setting up and running the GENESIS sediment transport model was provided by Lee Butler of Veri-Tech, Inc I am very grateful for his patience and professionalism.

Support for this research was provided by the National Oceanographic and Atmospheric Administration Coastal Services Center (NOAA Award No.

NA960C0308), the State of Hawaii Department of Land and Natural Resources- Marine Resource Initiative (Award No. 432545) and the Hawaii Sea Grant College (Award R/EP12). Additional thanks goes to the UGGS for their support with surveying equipment and advice on technical questions.

Last but not least I thank my family, especially my wife Malia for her unconditional support, understanding and encouragement during times of frustration and self-doubt as a student.

ABSTRACT

Using monthly beach profile surveys and historical aerial photographs, the seasonal and long-term (48 year) beach morphology for Kaanapali Beach, Maui is described. By identifying the shoreline position in historical aerial photographs it is determined that the Kaanapali area is subject to long periods of mild erosion and accretion punctuated by severe erosional events related to short-period Kona storms and hurricane waves. Increased Central Pacific tropical cyclone activity of the late 1950's and early 1960's and Hurricane Iniki in 1992 are identified as contributing factors to the observed volume change during these periods. Between these erosional periods the Kaanapali shoreline is relatively stable characterized by light erosion to moderate accretion suggesting the recovery time may be on the order of roughly 20 years.

Over the 48-year period 1949 to 1997, the Kaanapali and Honokowai cells have experienced a net sediment volume loss of 43,000 ±730 m^3 and 30,700 ±630 m^3 respectively for a total net volume loss of 73,700 ± 990 m^3. The Kona storms and hurricanes of the early 1960's and 1992 collectively account for 136,000 m^3 of sediment lost or approximately 62% of the gross volume change for the entire period, revealing the significant erosional effect of these storms. Recovery after each of these storms accounts for 73,900 m^3 or approximately 33% of the gross volume change. A residual loss of 10,600 m^3 representing 5% of the gross volume change is inferred as chronic erosion and may be a product of relative sea-level rise (RSLR). An increase in short-period southwesterly wave energy during these erosional periods is well documented and may have transported beach sediment further offshore than normal (beyond the reef) and is identified as a possible mechanism for long-term erosion in this area.

The spatial distribution of historical shoreline movement suggests the majority of sediment transport occurs in the central portion of Kaanapali near Kekaa and Hanakoo Point and is driven by longshore rather than cross-shore transport.

Surveyed beach profiles reveal a strong seasonal variability with net erosion in the summer and accretion in the winter with an along the shore-alternating pattern of erosion and accretion. 65% of the net volume change occurs south of Kekaa Point confirming the more dynamic nature of the southern (Kaanapali Cell). Net beach profile volume change from the mean suggests that June and January are the most dynamic months each with approximately 14% of the total volume change. We attribute the significant and rapid erosion and accretion events due to wave-induced longshore transport of sediment.

Field observations of monthly beach sediment impoundment in the Kaanapali cell are examined and compared to three models that predict longshore sediment transport (LST). Beach profile results indicate sediment impoundment occurs seasonally with a nearly balanced longshore sediment transport system between profile 5 and 9. Longshore transport rates are derived from seasonal cumulative net volume change in the middle of Kaanapali Beach at profile 7. Cumulative net sediment transport rates are 29,379 m^3/yr ± 15% to the north and 22,358 m^3/yr ± 6% to the south for summer and winter respectively, a net annual rate of 7,021 m^3/yr ± 10% to the north and a gross annual rate of 51,736 m^3/yr ± 2%. Predictive transport formulas such as CERC (1984), CERC (1991) and

Kamphius (1991) predict net annual transport rates at 3 x 10^3 percent, 77 percent and 6 x 10^3 percent of the observed transport rates respectively.

The presence of fringing reef significantly effects the ability of the LST models to accurately predict sediment transport. When applying the CERC (1984, 1991) and Kamphius (1991) formulas, the functional beach profile area available for sediment transport is assumed much larger than actually exists in Kaanapali because of the presence of a fringing reef that truncates a portion of the sandy profile area. The CERC (1984, 1991) and Kamphius (1991) formulas don't account for the presence of a reef system which may contribute to the models overestimate of longshore sediment transport as they assume the entire profile is mobile sediment. However the fact that the CERC (1991) model underestimates the observed transport implies that additional environmental parameters (such as wave height, direction and period) play a more substantial role than the influence of the reef in the model results.

The CERC (1991) Genesis model is found to be superior in fitting the observed longshore transport at Kaanapali Beach. The success of the Genesis model is partly attributed to its' ability to account for short-term changes in near-shore parameters such as wave shoaling, refraction, bathymetry, antecedent conditions and several other shore face parameters not accounted for in the CERC (1984) or Kamphius (1991) formulas. The use of the CERC (1984) formula is prone to practical errors in its' application particularly in the use of the recommended "*K*" coefficient and wave averaging that may a significantly overestimate the LST. A better fit to the observed LST is achieved with the CERC (1984) if the *K* value is decreased by an order of magnitude from 0.77 to 0.07. The Kamphius (1991) formula is especially sensitive to extremes in wave period and tends to deviate from observed transport estimates for unusually high wave periods (this study) and approximates observations nicely in areas with low wave periods (Ping Wang *et al.* (1998)).

Many of the studied predictive LST formulas are prone to overestimate transport and thus their use requires a comprehensive understanding of the complexities and errors associated with employing them. Great care must be used when applying LST models in areas with significant hard bottom or shallow reefs that alter the beach profile shape. Due to these errors, the use of the CERC (1984) and Kamphius (1991) formulas are better suited as a qualitative interpretative tool of transport direction rather than magnitude.

TABLE OF CONTENTS

LIST OF TABLES

LIST OF FIGURES

1. INTRODUCTION

Beaches have always been a central part of the lifestyle and economy of Hawaii. Hawaii is susceptible to many natural hazards including coastal erosion (Richmond, *et al.*, 2001). Many coastal studies indicate that erosion is widespread and poorly understood in Hawaii (Sea Engineering, Inc., 1988; Makai Ocean Engineering, Inc. and Sea Engineering Inc., 1991; Fletcher, *et al.*, 1997, Fletcher and Lemmo, 1999, Fletcher, *et al.*, 1994; Rooney and Fletcher, 2000; Richmond, *et al.*, 2001). Eroded shorelines are more vulnerable to natural hazards and increase the risk to coastal development. Eroded beaches are not able to buffer storm waves, eustatic sea-level rise and marine flooding thus threatening existing and proposed coastal development (Fletcher, *et al.*, 1997). To enhance management of natural hazards and coastal resources it is important to gain a better understanding of the seasonal and long-term coastal dynamics in Hawaii and to quantify the response of the shoreline to critical environmental parameters.

Predicting rates of longshore and cross-shore transport is the subject of many coastal science and engineering studies. Most modern predictive sediment transport formulas is largely empirical and reflects results based on field studies from around the world (Komar and Inman, 1970; Dean., 1989; Kraus, *et al.*, 1991; Short, 1999). Field techniques for measuring total and suspended longshore sediment transport include sediment tracer, impoundment and streamer traps. Here we employ the impoundment technique for comparison with three predictive longshore transport models

The seasonal and long-term beach morphology for Kaanapali Beach, Maui is described. The complex and irregular near-shore sediment transport system is examined using 13 monthly beach surveys and the historical sediment volume history based on the

shoreline position in aerial photographs over a 48 year period (1949 to 1997). The dominant spatial and temporal patterns of sediment transport and volume variability is described and we evaluate three commonly used Longshore Sediment Transport (LST) formulas: (CERC, 1984; Kamphius, 1991; and The Army Corps of Engineers (ACOE) Generalized Model For Simulating Shoreline Change (*GENESIS*) model CERC, 1991). Each of these transport formulas is compared with observed sediment transport rate measurements in Kaanapali Beach, Maui.

The CERC, (1984) and Kamphius, (1991) predictive LST formulas are prone to overestimate the observed longshore transport by roughly an order of magnitude and thus their use requires a comprehensive understanding of the complexities and potential errors associated with employing them. The presence of fringing reef may effect the ability of these LST models to accurately predict sediment transport, however the fact that the CERC, (1991) model underestimates the observed transport implies that additional environmental play a more substantial role in the model results. The CERC, (1984) and Kamphius, (1991) formulas are better suited as a qualitative interpretative tool (when used in addition to other LST formulas) of transport direction rather than magnitude due to the potential errors and inaccuracies of using an uncalibrated transport formula.

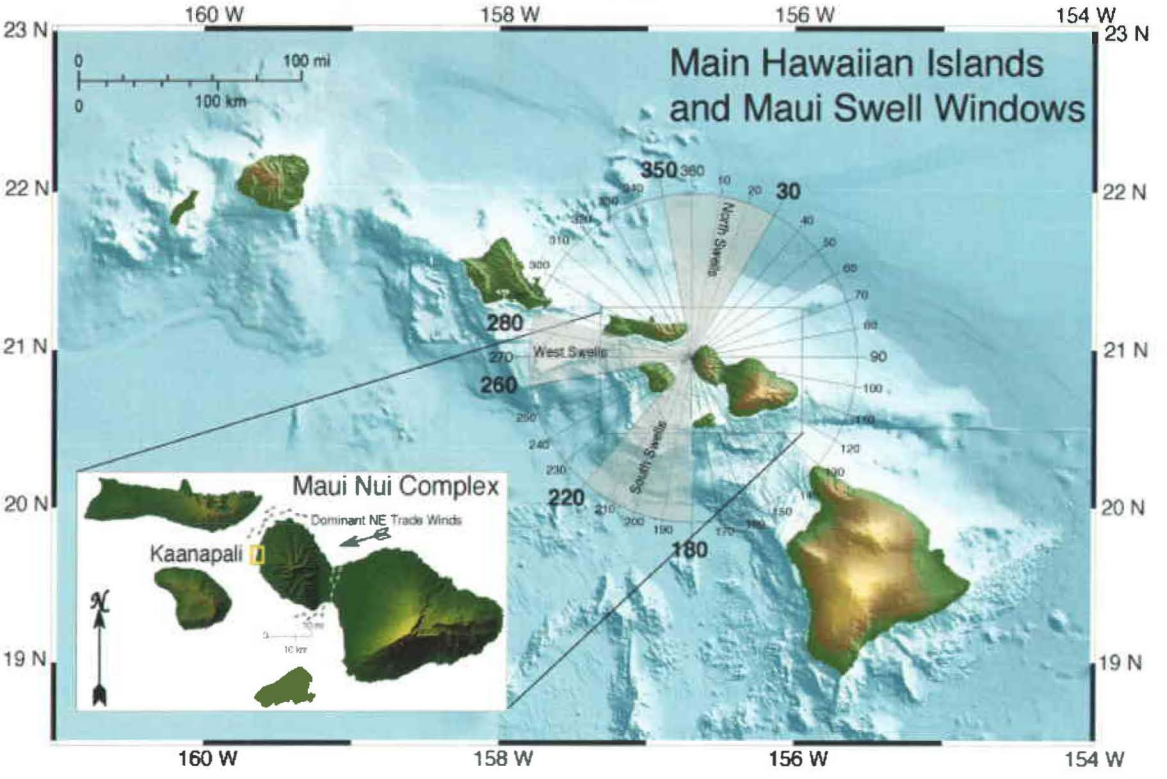

Figure 1. Kaanapali Location Map and Swell Windows

2. ENVIRONMENTAL SETTING

Kaanapali Beach is located on the west coast of the island of Maui, Hawaii in the lee of the dominant northeast trade winds (Figure 1). Environmental conditions on this coast are typically calm with side shore trade winds and infrequent but strong onshore storm winds (Kona Storms). Tidal-driven, surface currents are dominantly from south to north along the offshore portion of this coast and can exhibit strong currents due to the shallow bathymetry between Maui and Lanai. Wave-driven, near-shore currents are seasonably variable but are generally restricted to a shore-parallel north-south or south-north trend. The surrounding islands shelter the area from long period swell except for three pronounced swell windows. The southern swell window ranges from approximately

180° to 220°, the west swell window from 260° to 285° and the northern swell from 350° to 30°.

The beach system experiences seasonal wave forcing from north and south directions, while west swell events are rare. North Pacific swells in the winter months can exceed 10 m in height with periods of up to 25 s. South swells are commonly 1 to 3 m but can exceed 5 m in height and with periods of up to 22 s (Armstrong, 1983). Kona storms are low-pressure systems that cause strong local winds from the south or southwest. Kona storms can generate wave heights up of 3 to 5 m and periods of 8 to 10 s. Although these storms occur infrequently, they are the main cause of extensive coastal damage to south and west facing shorelines (Makai Ocean Engineering, Inc. and Sea Engineering Inc.,1991; Rooney and Fletcher, 2000). Hawaii has a semi-diurnal tide with an annual range of 0.8 m. Significant wave heights (mean of highest third) range from 2.5 m to 1.85 m for winter and summer respectively (Juvik, 1998).

Geophysical investigations suggest the Hawaiian Island chain is undergoing variable rates of uplift and subsidence. Tide gauges indicate the rates of subsidence decrease exponentially away from the hotspot located just south of the Big Island. Lithospheric flexure is postulated to be a driving force in the variable uplift rates in Hawaii with the Molokai, Lanai and Oahu undergoing a slight degree of relative uplift (Grigg and Jones, 1997). Tide gauge data indicate that Kahului Harbor, Maui is experiencing a relative sea-level rise of 2.46 cm/decade ±0.23 cm which is 40% greater than that on Oahu or Kauai, presumably due to more pronounced subsidence in East Maui than Oahu and Kauai (Fletcher, 2002).

The study area consists of a 4,600 m continuous carbonate beach that is bisected by the prominent basalt headland Kekaa Point also commonly known as "Black Rock" (Figure 2). Kekaa Point divides the area into two distinct littoral cells, the Honokowai cell to the north and the Kaanapali cell to the south. These two cells are evaluated separately with no significant exchange of sediment between the cells. The focus of this study is centered on the northern portion of the southern (Kaanapali) cell between profiles 5 and 9. This is the most dynamic portion of the study area with a well-defined seasonal sediment transport component. High-density coastal development exists in the Kaanapali Cell with at least 12 major beach side resort hotels between Kekaa Point and Hanakoo Point. Additionally there is extensive condominium development from Honokowai Point north as well as a new condominium complex currently being built near Kahekili Beach Park (profile 3).

Figure 2. Kaanapali fringing reef, channels and beach survey locations.

The beach is composed of moderate to well-sorted coarse carbonate sand with a minor basalt component and a median grain size diameter of 0.23 mm. Beach sand increases in basalt percentage nearing Hanakoo Stream in the southern portion of the study area (Inman and Waldorf, 1978). The beach generally

displays a steep foreshore slope range (vertical : horizontal) from 1:5 to 1:15 (mean 1:8), and a gentle backshore (subaerial) slope ranging 1:5 to 1:17 (mean 1:10). The Kaanapali and Honokowai nearshore generally exhibit a reflective beach state with plunging to surging waves (Wright and Short, 1984). This beach state is associated with coarser sediments and generally displays a steep narrow beach with a well-defined toe at the base of the foreshore. The strong swash and coarse sediment often develop pronounced subaerial beach cusps. Occasionally the area will fluctuate between the reflective and intermediate transverse bar and beach with surging waves. In this state, crescentic attached beach cusps (megacusp horns) form longshore and segregate individual rip systems approximately every 100 m.

A shallow (<1 m deep) fringing reef dominates the northern and southern extents of the study area with deeper outcrops of fossil reef (5-10 m depth) observed intermittently in the central area between profiles 5 and 8. The fringing reef is underlain by fossil reef and beachrock that dominates the reef flat and shallow reef segments. Encrusting coralline algae and branching corals are found at deeper regions of the reef front forming spur and groove features in the reef slope at depths of 10-20 m. At approximately 500 m intervals, the fringing reef is broken by shore-normal channels (Aawa) that direct the flow of nearshore water and sediment seaward.

The fringing reef constitutes a geologic framework that plays a significant role in the stability and replenishment of the beach system in this area. The Southern Kaanapali area is largely fronted by fringing fossil coral reef that restricts the sub aqueous beach profile area actively involved in sediment transport and can be idealized as a perched beach atop

a fossil reef. This shallow fringing reef truncates the surface area of the beach profile, reducing the total area that is available for sediment exchange.

3. PREVIOUS WORK

3.1 Previous Beach Profile and LST Studies

Wright and Short, (1984) examined the morphodynamic variability of beaches and surf zones of eastern Australia. They created a widely used beach classification method based on breaking wave height (H_b), period (T) and grain size, as defined by sediment fall velocity, (W_s) commonly defined as the Dean Parameter $\Omega = H_b/W_sT$. They found that when $\Omega<1$ beaches tend to be reflective, when $\Omega>6$ they tend to be dissipative.

Munoz-Perez, *et al.*, (1999), present a beach equilibrium profile model for reef-protected beaches of the Spanish coast. They examined wave decay due to shoaling over a hard substrate and its effect on the shape parameter used in the equilibrium profile model of Dean, (1977). They concluded that no equilibrium beach profile is possible within a distance of 10 to 30 units x h_r from the edge of the reef, where h_r is water depth over the reef.

The sediment impoundment technique (sediment blocking by a structure) has been successfully used to estimate longshore sediment transport (LST) (Johnson, 1957; Bruno and Gable, 1977; Bodge, 1987; Dean, 1989). In this technique, the volumetric transport rate is estimated from the sediment volume change on the updrift side of a temporary blocking structure.

Ping Wang, *et al.*, (1998) measured longshore sediment transport from streamer traps at 20 locations along U.S. East and Florida Gulf coasts. They concluded that longshore

sediment transport on low energy coasts was considerably lower than predicted by published empirical transport formulas. They found that Kamphius, (1991) predicted sediment transport three times lower than the commonly used CERC, (1984) formula and approximated the measured transport. Ping Wang, *et al* (2002) further examined LST in the Large-Scale Sediment Transport Facility (LSTF) at the U.S. Army Engineer Research and Development Center. Here they measured the change in sediment transport due to wave type and concluded that sediment transport was an order of magnitude higher during plunging waves than spilling.

Moberly, *et al.,* (1963, 1964) and Gerritson, *et al.*, (1978) carried out beach profile surveys of selected beaches on Oahu and produced the first record of beach profile change in Hawaii. Inman and Waldorf, (1978) conducted a beach and reef survey in Kaanapali, Maui where they documented sediment composition and geologic framework as well as developed a simple nearshore circulation model. They concluded that reefs play a significant role in the stability of the shoreline in Kaanapali and that no attempt should be made to alter the reef for a proposed swimming area. Dail, *et al.*, (1999) measured seasonal beach morphology changes at Waimea Bay, Oahu using RTK-GPS and video analysis of shoreline wave run up. They found a high correlation (-.88) of wave energy flux to beach volume using a filtered wave energy formula that integrates antecedent wave conditions for determining beach state over a 16 month period.

Bodge and Kraus, (1991) examined several inconsistencies in the practical application of the CERC, (1984) formula and conclude that errors in field measurements and formula expressions can potentially yield errors in the LST formula by a factor of 2 to 15. Due to an a prevailing overestimate of the LST by the CERC formula, the use of

the suggested empirical (K) coefficient of 0.77 must be modified for practical applications. Reduction of (K) by an order of magnitude was found to yield more reasonable results (Ping Wang *et al.* 1998; Bodge and Kraus, 1991). This was found to be especially true on coarse, poorly sorted beaches such as Kaanapali Beach.

Sea Engineering , (1996) carried out a design and planning study examining the historical rates of accretion and sediment transport for Kikiaola Harbor on the west coast of Kauai using sediment traps and empirical formulas. They found gross sediment transport measured from sediment traps to be ~40,000 m^3/yr for calm wave conditions. Using the CERC, (1984) formula they calculated a gross annual sediment transport rate of 1,688,900 m^3/yr. Recognizing the CERC (1984) wave power coefficient was empirically derived from U.S. continental dissipative beaches, Sea Engineering determined a new wave power coefficient (K) roughly and order of magnitude smaller using data from Hawaiian beaches and calculated a gross annual transport rate of 269,880 m^3/yr.

3.2 Previous Aerial Photogrammetry and Shoreline Analysis Studies

Smith and Zarillo, (1990) attempted to quantify seasonal error resulting from shoreline calculations based on aerial photographs. They found that seasonal fluctuation of the shoreline might be the single largest source of variability when calculating long-term change of the shoreline. Coyne, *et al.*, (1999) developed an end-point analysis to calculate historical shoreline change based on orthorectified aerial photographs.

Modifying the procedure of Coyne, *et al.*, (1999), Rooney and Fletcher, (2000) performed a time series analysis of historical beach volume change using aerial photographs and seasonal beach surveys for a 5 km segment in Kihei, Maui. They found a regional pattern in the sediment budget where net volume gain in the northern portion of the study site far exceeded net sediment loss in the southern portion. They concluded that significant coastal erosion results from the frequency of local Kona Storms, which in turn correlates to the Pacific Decadal Oscillation (PDO). Norcross, *et al.*, (in press) looked at the dominant spatial and temporal patterns of beach morphology at Kailua Beach, Oahu, Hawaii. They identified large-scale beach meanders exhibiting an alternating pattern of erosion and accretion longshore in response to the seasonal wave state. They also document net accretion of 673,000 m^3 from 1926 to 1996 and suggest an offshore sediment source for this accretion.

4. METHODOLOGY

4.1 Seasonal Beach Morphology

4.1.1 Monthly beach surveys

Monthly beach profile observations were collected at 11 shore-normal transects situated along the length of the study area (Figure 3). Thirteen monthly surveys were performed from March, 2000 to April, 2001. Surveys were conducted randomly with respect to tide and swell conditions. Beach profiles were measured using a Geodimeter ® Total Station and a 7 m telescoping rod with prism. The surveys were carried out on a shore-normal transect over the sub-aerial and sub-aqueous portions of the beach. Measurements of the X, Y and Z position were obtained at approximately 2 m intervals or at each significant change in slope or bottom type. The profiles extend from the landward toe of the dune system (where present) beyond the beach toe to the edge of the reef slope.

Monthly beach volumes are calculated as the area under the profile extending from the landward edge of the beach to the first occurrence of hard substrate or depth of closure (DOC) often just beyond the toe of the beach (Figure 4). The sand/reef interface at each profile is used as the lower depth limit of each volume calculation and is assumed to extend horizontally landward from its' first occurrence. Profile volumes are calculated as sectional volumes assuming a 1 m wide profile section (X m^3/m) which is in-turn multiplied by the longshore distance represented by each profile to achieve total volume of that area (X m^3).

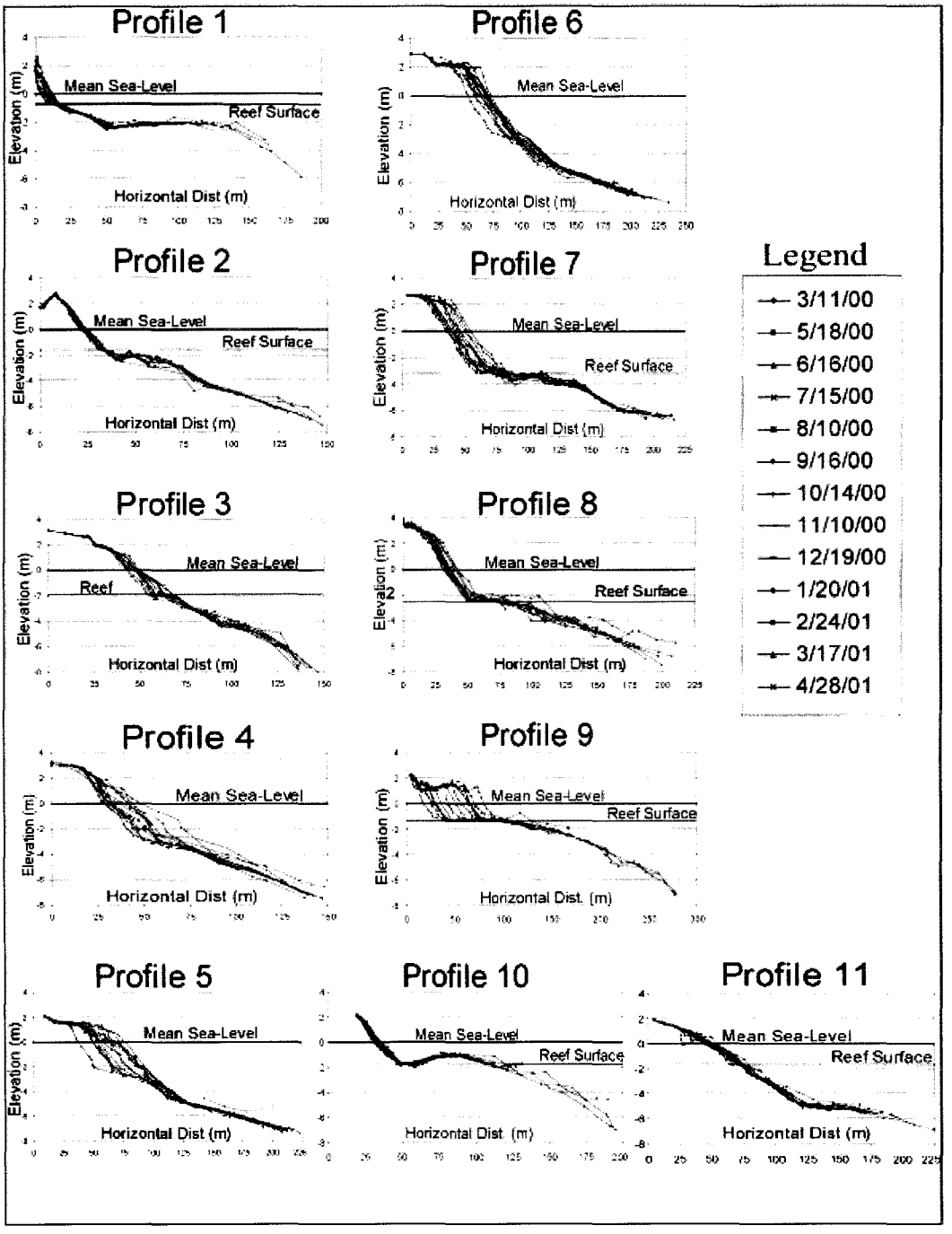

Figure 3. Monthly beach profiles. Profile 1 is located in the north and 11 in the south. Note seasonally uniform cross-shore profile shape.

4.1.2 Depth of Closure (Sediment-Reef Interface)

In carrying out the beach profile surveys, continuous and patch hard reef was encountered along many of the profiles in Kaanapali. The presence of a fringing reef significantly alters the beach profile by truncating that portion of the beach and creating a shallower than expected sand-reef interface, often referred to as the depth of closure (DOC). The first occurrence of hard substrate is considered the depth at which the profile is no longer adjusting to wave energy and sediment remains stable and hence operates a prescriptive DOC. In Kaanapali, we find a shallow DOC where there is reef present and a deeper DOC where the profile remains sandy.

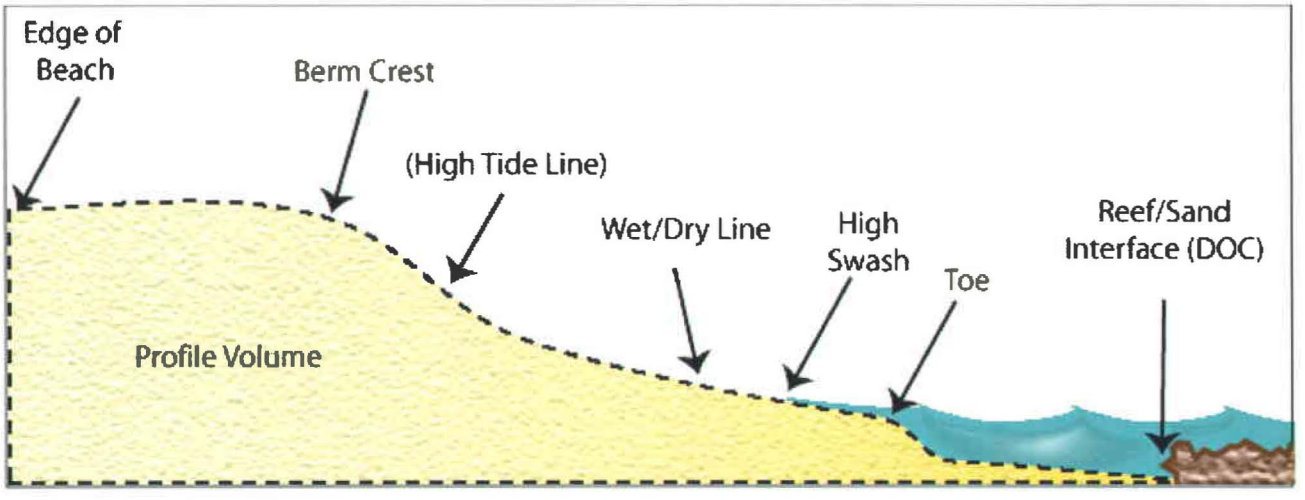

Figure 4. Shoreline and beach profile features.

4.2 Historical Shoreline Change

4.2.1 Aerial Photogrammetry

Historical shoreline positions identified on aerial photographs and NOAA Topographic sheets provide an 89-year history (1912 to 1997). Only 1:12,000 scale or larger, vertical, survey-quality aerial photos were used. Photo years included: 1949, 1961, 1963, 1969, 1975, 1987, 1988, 1992 and 1997. Two NOAA Topographic sheets (T-Sheets) were used (1912 and 1932) to extend the historical coverage. Volume calculations are derived only from 1949 to 1997 photo sets as the T-Sheets do not delineate the position of the vegetation line. Scanned images were orthorectified (geo-spatially oriented and fit to a coordinate reference system), adjusted for rectification errors (Thieler and Danforth, 1994) and mosaicked following the methodology of Coyne, *et al.*, (1999). The uncertainty associated with this process is discussed in more detail in Section 5.6.

Orthorectifed photo mosaics contain vectored shorelines with a common scale of 1:3000, a pixel size of 0.5 m and a UTM referencing in the WGS 84 Datum. To calculate erosion and accretion rates and document historical changes in beach width the toe of the beach and the vegetation line are identified as the seaward and landward delineations of the beach respectively. Historical movement of the shoreline is tracked using the toe of the beach as described by (Coyne, *et al*, 1999; Rooney and Fletcher, 2000; and Norcross, *et al.*, in press). Each shoreline vector is overlain on the 1997 photo mosaic and a time series of shoreline movement is calculated (Figure 5) as described by Crowell, *et al.,* (1999). Rates of shoreline change are calculated using a re-weighted least

squares linear regression (RLS) of the position of each shoreline at an longshore spacing of 20 m.

Figure 5. Example subset image of Kaanapali region. Shown are shoreline vectors and 20 m transect intervals used in calculating the rate of shoreline change plots shown here in red (units in meters).

4.2.2 Historical Volume Change

To estimate historical beach volumes we apply a volumetric change model established by Bodge, (1998) and modified by Rooney and Fletcher, (2000); and Norcross, *et al.*, (in press). In this model, historical beach volume flux is estimated from historical beach widths measured from aerial photos. This model is based on the relationship of the change in beach volume (dv) to the change in the position of the beach width (dx) as observed in the 13 monthly beach surveys for 11 individual beach profiles (Equation 1 and Figure 6). In the dv/dx model, the slope of the regression line fit to the profile data and run through the origin, provides us with a "G_p" value, expressed as:

$$G_p = \frac{\Delta V}{\Delta X} = \frac{\text{Volume change per unit of shoreline}}{\text{Change in beach width}} \qquad \textbf{(1)}$$

The slope of G_p is applied to the value ΔX on each transect spaced 20 m longshore at the study area. The historical beach volume change ($\Delta X * G_p$) provides the volume change per meter of shoreline (m^3/m) and comprises the first term in the volumetric change model (Equation 2 and Figure 7). The second term ($\Delta Veg * \Delta Z$) reflects the change in volume associated with the movement of the vegetation line. The first component, ΔVeg is the horizontal change in the position of the vegetation line observed on the aerial photographs. The second component of this term ΔZ, is the elevation above the depth of closure or reef surface at the seaward position of the vegetation line as measured in the monthly beach profile surveys. The vegetation volume change is defined as the product of ($\Delta Veg * \Delta Z$) and describes the change in volume under the back beach vegetation as a result of historical movement of the vegetation line. Thus a

seaward movement of the vegetation line would increase the volume of the vegetation component and reduce the beach volume component.

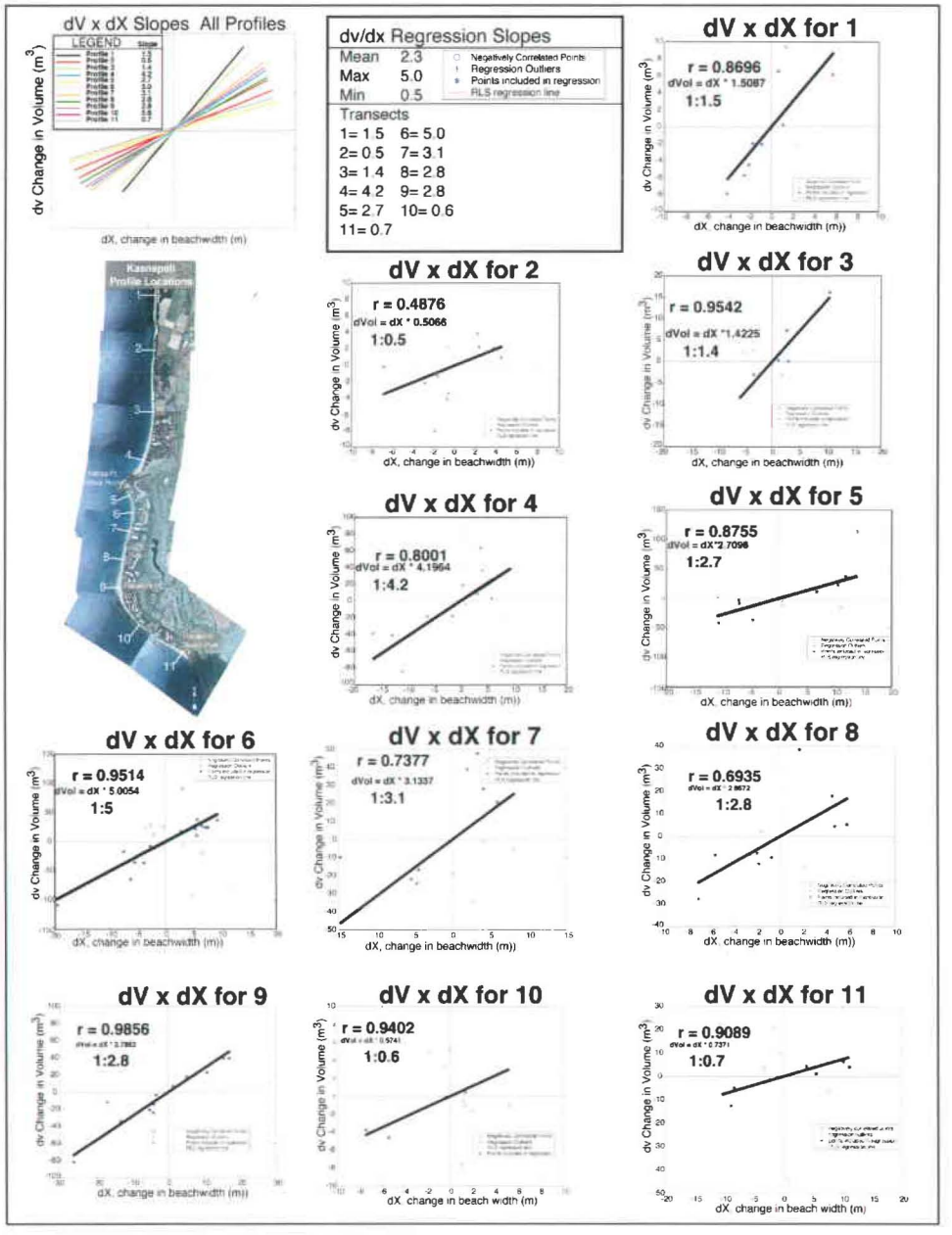

Figure 6. Modern dv/dx slopes applied to calculate historical volume change. A separate dv/dx plot is produced for each profile. A linear regression line is run through the data points, the slope of the line calculated and the r-value of the data correlation calculated for each plot.

Here we combine the beach volume and vegetation volume terms to define the total change in volume (ΔVol_{total}) and can be written as follows:

Volume Change Model:

$$\Delta Vol_{total} = [(\Delta X * G_p) + (\Delta Veg * \Delta Z)] * 20\ m \quad \text{Where:} \qquad (2)$$

ΔVol_{total} =	Total change in beach volume per unit of shoreline (m^3/m)
ΔX =	Horizontal change in beach width (m) (BW1-BW2).
G_p =	Slope of the best-fit line from the $\Delta V/\Delta X$ plot.
ΔVeg =	Horizontal change in the vegetation line (m).
ΔZ =	Elevation of the vegetation line above the depth of closure (m).

We multiply equation 2 by 20 meters to represent the area covered by each transect. Summing all the transect volumes and dividing by the time between each aerial photo (see section 4.2.1), we calculate a total volume change per year for the entire study area for each time period (m^3/yr). The net volume change for each transect is subsequently calculated by summing all the time periods for that transect.

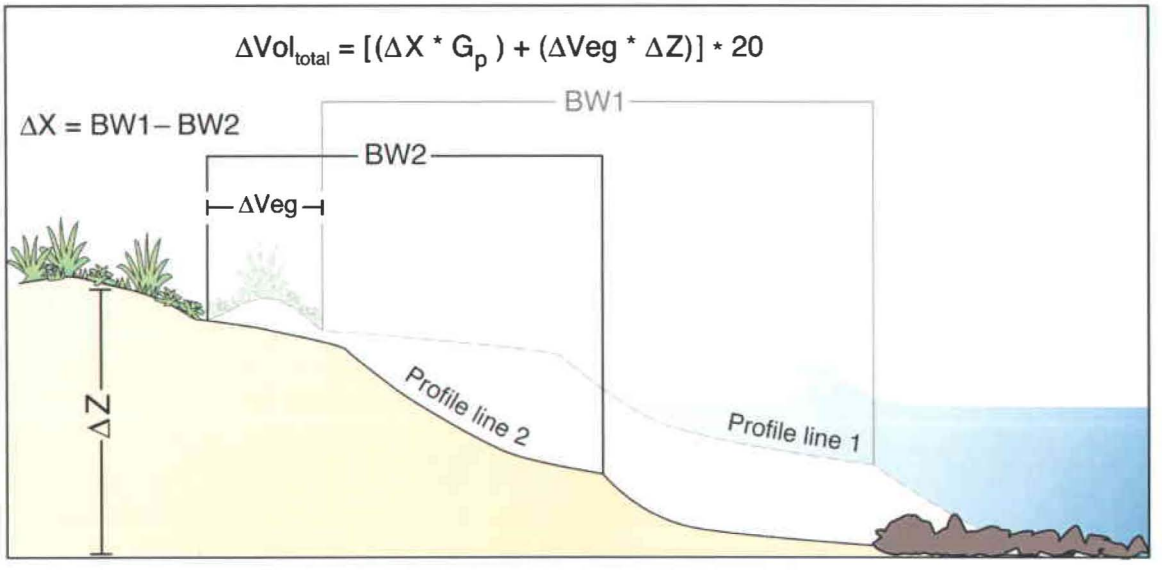

Figure 7. Volumetric Change Model (From Rooney and Fletcher, 2000)

4.3 Wave Data

Wave parameters such as height, period and direction are utilized for transport model input parameters and were obtained from two different sources. We specify the wave energy flux for Kaanapali based on offshore buoy data and coastal observations. For north swells we use wave data provided by the Coastal Data Information Program (CDIP) at the Scripps Institute of Oceanography for the Mokapu Datawell Waverider buoy #98, located at 21° 24.900 N 157° 40.700 W offshore from the Mokapu Peninsula, Kaneohe, Oahu. For north swells, we use a data set of significant wave height, period and direction filtered to the dominant wave direction thus eliminating the effect of trade wind swell on the wave readings. For south swells we employ the National Oceanographic Atmospheric Administration (NOAA) data base for coastal surf observations for Oahu provided by National Oceanographic Data Center's (NODC) and the National Coastal Data Development Center (NCDDC) Hawaii/Pacific Liaison Office. This public-domain data set includes observed breaking wave surf heights and estimated direction for the south shore of Oahu and adequately approximates the south swell exposure of the Kaanapali region. Seasonal wave data such as height, period and direction from these sources are applied as input to the (CERC 1991) wave refraction model and then run in the LST models discussed below.

4.4 EOF Analysis

Empirical Orthogonal Function (EOF) analysis is applied to quantify temporal and spatial modes of variability in monthly profiles and historical shoreline positions. EOFs are used to reduce the number of data variables for a specific data set and are derived

from sample covariance estimates so the structure of the functions are defined by the actual data set. The functions are orthogonal, each function representing a portion of the mean square value of the data. Each mode is uncorrelated in the spatial and temporal domain and are useful in highlighting underlying patterns of variability that are otherwise difficult to interpret (Winant, *et al.*, 1975, Aubrey, 1979; Dick and Dalrymple, 1984). We use EOF analysis to isolate the spatial and temporal patterns of both seasonal profile change and historical shoreline position. Discussion is focused on mode 1 variability as it represents the dominant form of variability within the study area.

4.5 Near-shore Sediment Production

Calcareous reef-dwelling organisms such as foraminifera, red algae, mollusks, coral and echinoids are the dominant contributors of littoral sediment production in the study area (Moberly, *et al.*, 1963). The fringing reefs in the north and south extents of the area provide a small portion of the modern calcareous sediment delivery to the beach. Older sand stored in deeper water, pockets in the reef and along the shoreline, is transported longshore and eventually a portion of this sediment is delivered to the beach. A minor source of sediment is derived from the Hanakoo stream at the far southern extent of the area. The component of volcanically-derived terrestrial sediment increases significantly at the Hanakoo stream mouth. As much as 81% of the beach sediment is reported to be terrestrial fronting the stream mouth (Inman and Waldorf, 1978). Estimates of longshore sediment transport can be made from the gradient of terrigenous to calcareous beach sediment from the origin at the stream mouth. Inman and Waldorf, (1978) estimate the

longshore transport rate for the south Kaanapali area to be 1000 m^3/yr with an annual influx of carbonate sediment of 3.5 m^3/m.

Gross calcium carbonate production rates for Kailua Bay, Oahu range from 1.4 to 7.0 kg/m^2/yr for the reef flat and slope respectively of which only 25% of the reef flat and 12.5% of the reef slope gross $CaCO_3$ production is estimated to be available to the beach (Rooney and Fletcher, 2000). Although the Kaanapali area is in a different reef ecosystem than Kailua Bay, Oahu, gross $CaCO_3$ production is estimated to be very similar. Three areas of modern $CaCO_3$ sediment production within the study area are identified, the Honokowai Reef (75,000 m^2), the Kahekili Reef (40,000 m^2) and the Hanakoo Reef (80,000 m^2). We estimate gross $CACO_3$ production to be 1.2 kg/m^2/yr and a sediment density of 1176 kg/m^3 (Harney, *et al.*, 1999). Thus gross $CaCO_3$ delivery to the beach is approximately 77 m^3 /yr, 41 m^3 /yr and 82 m^3 /yr for the Honokowai, Kahekili and Hanakoo Reefs, respectively, for a total sediment delivery from nearshore reef production of approximately 200 m^3 /yr.

4.6 Longshore Sediment Transport

By examining the seasonal sediment volume exchange between profiles 5 and 9, we find that the dominant direction of sediment transport for the Kaanapali area is longshore. Beach profiles exhibit little to no cross-shore transport of sediment but they do show a significant change in beach face profile volume, which suggests longshore transport. We use the cumulative volume change of profile 7 as a proxy for LSR because it represents the longshore location where seasonal cumulative volume trends reverse sign and represents a hinge point in the trend of the data. We compare observed net annual

longshore transport rates at profile 7 with the predicted transport rates of the CERC (1991) *Genesis* model, Kamphius (1991) and CERC (1984) longshore transport formulas in the same approximate location. We examine these comparisons in the following results section (5.7).

5.0 RESULTS AND DISCUSSSION

5.1 Short-term (seasonal) change

5.1.1 Regional Profile Volume Spatial Patterns

Surveyed beach profiles reveal a clear cyclic pattern of erosion and accretion due to seasonal wave forcing. While the profile volumes are variable along the shore we see that the mean volume, volume range and net volume are all significantly higher in the central portion of the study area and at Hanakoo Point at profiles 4,5 & 6 surrounding Kakaa Point and profile 9 (Table 1). The distribution of profile volume change clearly shows the dominance of the central portion of the study area and the clear decrease in mean profile volume away from the central area (Figure 8). We find that 65% of the net volume change occurs south of Kekaa Point confirming the more dynamic nature of the south (Kaanapali cell).

Further evidence of longshore sediment transport is derived from the net seasonal volume exchange between profiles 9 and 5. Observations of the net seasonal sediment volume change reveal a nearly balanced seasonal longshore sediment transport system with a balanced seasonal exchange of net sediment at profile 9 and profile 5. We attribute this seasonal volume change to sediment impoundment from longshore transport.

Table 1. Beach Profiles March, 2000 to April 2001

Profile	Maximum Volume (m^3/m)	Minimum Volume (m^3/m)	Volume Range (m^3/m)	Mean Volume (m^3/m)	Mean Volume Rate Change ($m^3/m/month$)	Net Volume Change (m^3/m)
1	29.23	9.26	19.97	18.26	-0.22	-2.83
2	94.71	83.37	11.34	87.64	-0.54	-6.97
3	137.80	112.17	25.63	128.35	0.99	12.91
4	**476.42**	**349.83**	**126.59**	**396.96**	**-7.50**	**-97.49**
5	**707.66**	**552.36**	**155.30**	**651.81**	**5.47**	**71.16**
6	**733.00**	**625.62**	**107.38**	**685.14**	**7.00**	**90.96**
7	379.11	244.52	134.59	317.91	0.33	4.24
8	222.70	165.94	56.76	185.64	-1.42	-18.44
9	206.82	45.88	**160.94**	126.47	-4.70	-61.15
10	107.13	92.16	14.97	98.50	-0.48	-6.18
11	305.80	261.58	44.22	283.22	0.35	4.50
Mean	309.13	231.15	77.97	270.90	-0.06	-0.84

Table 1. Surveyed beach profiles. Note increased mean volume, and volume range for the profiles in the central area surrounding Kekaa Point (in bold).

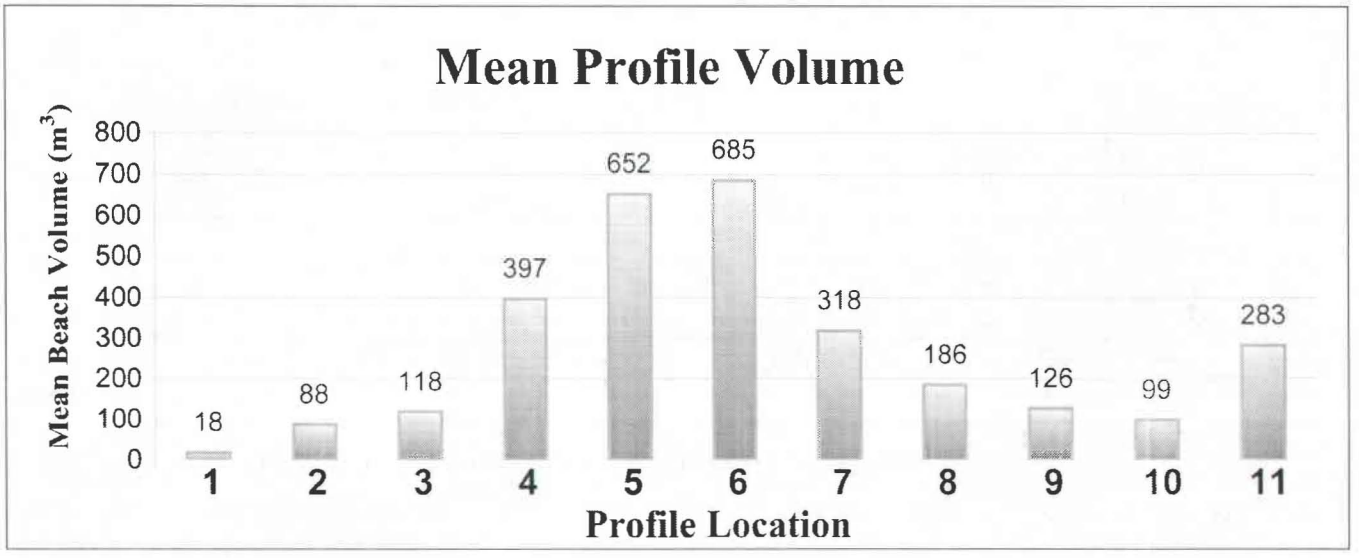

Figure 8. Mean profile volumes by location.

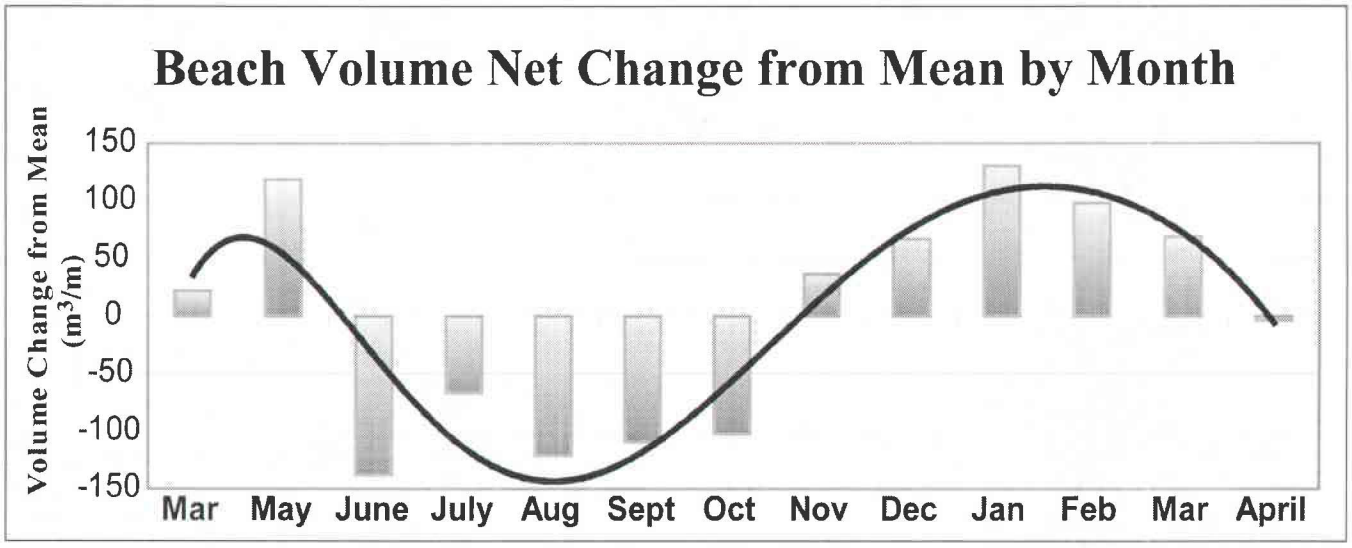

Figure 9. Monthly profile total net change from mean for all profiles showing trend line of best-fit polynomial regression. Note the clear seasonal pattern of erosion and accretion.

5.1.2 Profile Volume Temporal Patterns

Most profiles reveal a strong seasonal signal with net erosion in the summer and accretion in the winter for the entire area. A closer look at the total monthly change of profile volume suggests that the volume for each month is variable over the 13 month period with the peak summer and winter months showing the largest net loss or gain from the mean. From the monthly profile data the net volume change from the mean is calculated and suggests that June and January are the most dynamic months with approximately 14% and 13% of the total volume change respectively (Figure 9).

In addition to seasonal trends, an alternating pattern of erosion and accretion longshore is identified (Figure 10). Here the identification of the summer eroding profiles in red, the winter eroding profiles in yellow and a third pattern in white that are opposing each other and don't clearly fit into the previous two. The non-conforming

white profiles may be a function of temporary storage of sediment between seasonal states. The presence of such distinct alternating patterns of erosion and accretion suggests neighboring profiles exchange sediment seasonally and supports the theory that longshore transport dominates in this area.

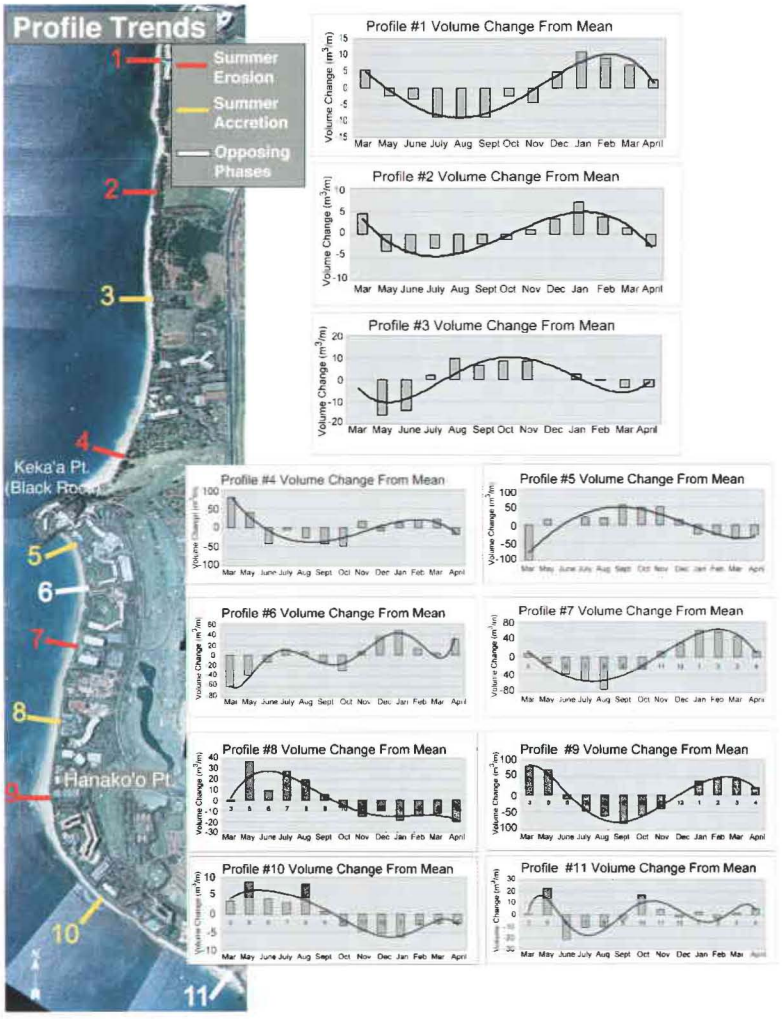

Figure 10. Beach profile trends. Note the alternating pattern of erosion and accretion as indicated by the alternating red and yellow transect colors. Volume plots to the right reveal the cyclic nature of the profiles as seen by the polynomial best fit (black) trend line.

A three-dimensional plot of profile volume change confirms a seasonal cyclic pattern and highlights the migration of erosion and accretion along the coast (Figure 11). The migration of sediment is idealized as 5 distinct phases during the 13 month study period. The horizontal axis of Figure 11 reveals an alternating pattern of erosion and accretion longshore from north to south for a given month while the vertical axis illustrates the seasonal pattern of erosion and accretion through time for a given shoreline position. We see the seasonal migration of erosion and accretion "hot spots" longshore as indicated by the arrows in Figure 11.

In the first phase of this migration we observe a southward migration of sediment in the spring from profile 5 to 9 (phase 1). Phase 2 depicts the onset of erosion during the summer months at profile 9. Phase 3 shows the migration of sediment northward from profile 9 to 5 as a result of increased summer, southerly swell. This is followed by continued delivery of sediment through the early winter months and the onset of erosion in the spring at profile 5 in phase 4. Phase 5 completes the annual migration cycle and conveys the southward migration of sediment in the spring from profile 5 to 9 as in phase 1. From Figure 11, we gain insight to the complex seasonal pattern of erosion and accretion of this region and observe the extent of seasonal sediment migration longshore through the various seasons.

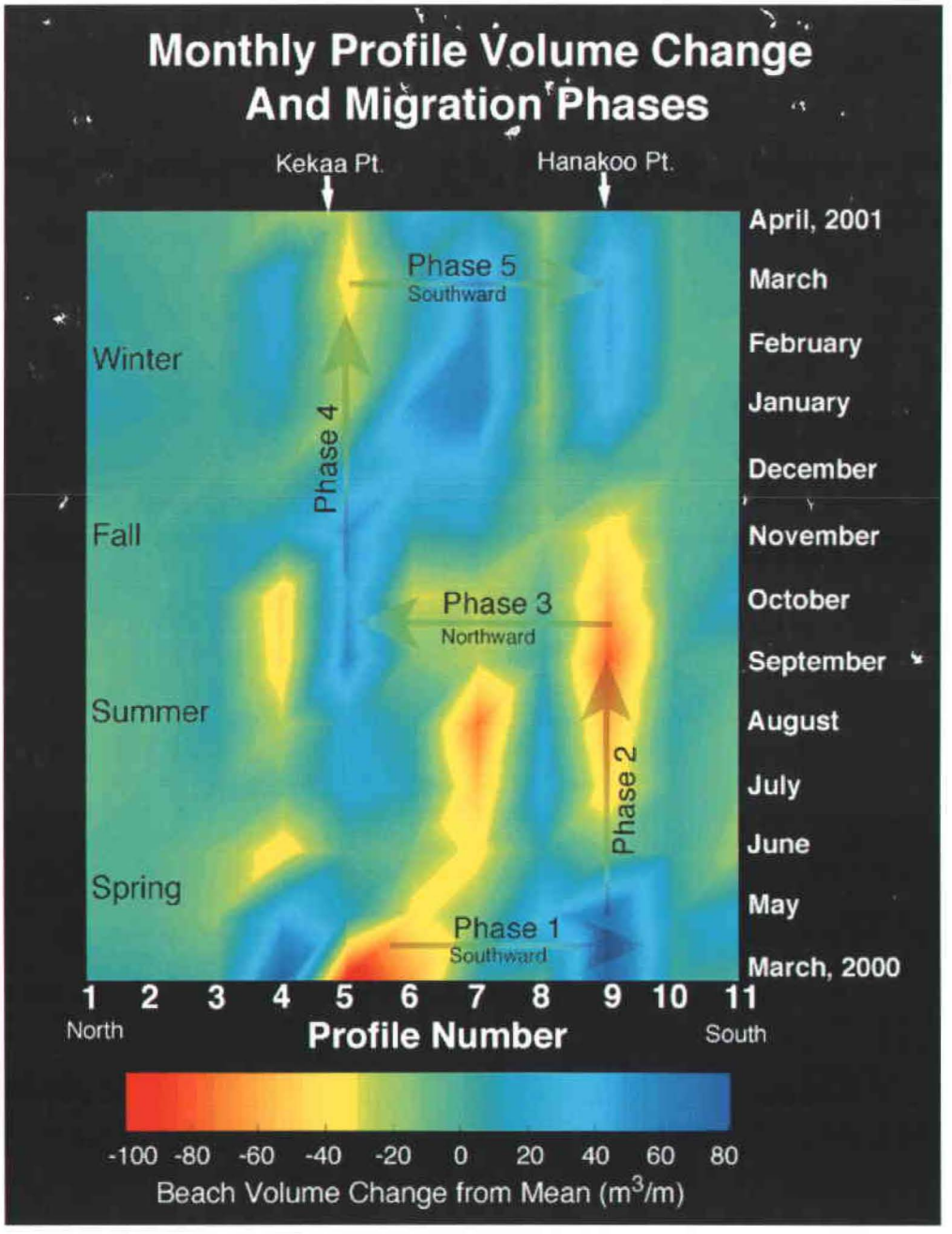

Figure 11. Three-dimensional plot of beach volume change from the mean. Note the sign reversal of volume change as the seasons change from summer to winter bottom to top. Arrows indicate the seasonal migration (phases) of erosion and accretion longshore through time.

5.1.3 Depth of Closure (Sediment-Reef Interface)

Beach profile surveys extend from the landward edge of the dune system (where present) beyond the beach toe to the edge of the reef slope. Shallow fringing reef is attached to the shoreline at profiles 1, 9 and 10 and significantly differs from the depth of closure predicted by Hallermeier, (1978) (Table 2). Where there is no reef present as in profiles 4 to 6, the actual depth of closure closer approximates the predicted depth. The calculated profile depth of closure (DOC) as defined by Hallermeier, (1978) is in most cases significantly deeper than the actual observed closure due to the presence of a shallow fringing reef (Figure 12). Predicted DOC is based on significant wave height and period (highest third of the wave data set) exceeded no more than 12 hours a year.

Table 2. Observed and Predicted Profile Depth of Closure

PROFILE	*Observed Depth of Closure (m)*	*Hallermeier Prediction (m)*
1	-0.70	-7.54
2	-1.80	-7.54
3	-2.10	-7.54
4	**-8.00**	**-7.54**
5	**-6.00**	**-7.54**
6	**-6.00**	**-7.54**
7	-3.00	-7.54
8	-2.50	-7.54
9	-1.20	-7.54
10	-1.70	-7.54
11	-2.30	-7.54

Table 2. Observed and predicted profile depth of closure (DOC). Note the deeper depth of closure at profiles 4-6 where there is no reef structure (bold).

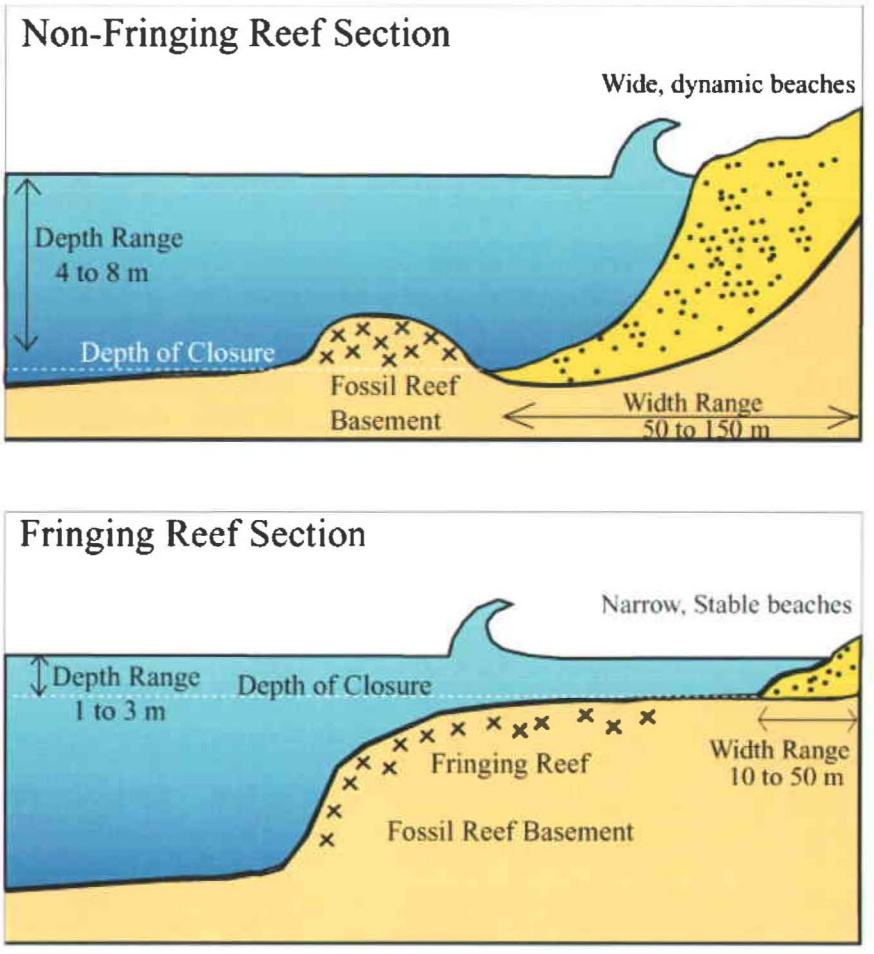

Figure 12. Non-fringing and fringing reef cross-section. We see a significantly shallower DOC where fringing reef is present.

5.1.4 Profile Volume Uncertainty

Three main sources of error in are identified in the uncertainty analysis for profile area volume. Where: Volume Uncertainty (*VU*)

$$VU = \sqrt{(\text{Meander Error})^2 + (\text{Basement Error})^2 + (\text{Cross-shore Error})^2}$$

Measurement error is considered negligible as the profiling technique used has centimeter accuracy. Likewise, the landward margin of the profile is fixed and thus induces no uncertainty. Meander error (± 500 m^3), is associated with variation in the seaward margin

of the sub-aerial profile as observed in foreshore meanders at the shoreline. Meander error is calculated by taking the mean observed meander width (±10 m) times the alongshore wavelength of the meander (50 m) times the profile area (1 m). Basement error (±2 m x 500 m x 1 m = ±1000 m^3), caused by variable relief of the basement strata, (which constitutes the lower boundary of the profile volume) is assumed to be horizontal landward from the first occurrence of hard basement. Cross-shore error (±1120 m^3), calculated from the seasonal profile net volume difference between profile 5 and 9, represents sediment lost outside the profile reach due to cross-shore transport. Using the additive error process described above, volume uncertainty for observed net annual volume change is estimated to be ±1100 m^3/month and is reported as the mean percentage of each monthly cumulative volume.

5.2 Historical Volume Change

5.2.1 Historical Photogrammetry results

Using a 85 year record of shoreline movement (1912 to 1997) an erosion rate for each transect (spaced 20 m apart) is calculated using two different regression models developed by Coyne and Fletcher, (1999) and applied by Rooney and Fletcher, (2000), and Norcross *et al*, (in press). End Point Rates (EPR) calculate the erosion rate based on the first and last known position of the toe of the beach. While the Annual Erosion Hazard Rate (AEHR) is a re-weighted least squares (RLS) linear regression that accounts for all the data points and reflects the more recent shoreline trend. Results show that the Kaanapali area has undergone a mean (AEHR) shoreline erosion rate of 0.3 m/yr (± 0.1 m/yr) and 0.1 m/yr (± 0.1 m/yr) for Honokowai (Table 3). Erosion rate uncertainty is

calculated from the residual error of the fit of the RLS regression line run through a plot of each historical position of the shoreline.

Table 3. Historical Shoreline Erosion Rates (1912 to 1997) (m/yr)

Regression Type	Mean Erosion Rate (m/yr)	Uncertainty ± (m/yr)	Maximum Rate	Minimum Rate
Kaanapali				
AEHR	-0.3	±0.1	-0.8	0.0
EPR	-0.3	-	-0.7	-0.1
Honokowai				
AEHR	-0.1	±0.1	-0.3	-0.4
EPR	-0.1	-	-0.3	-0.4

Using the volumetric change model described in section 4.2.2 , historical beach volumes are calculated. Both littoral cells reveal a net loss of sediment over the period 1949-1997 including a net loss of 30,733 ±630 m^3 for the Honokowai cell and 42,999 ±730 m^3 for the Kaanapali cell and a total net loss of 73,732 ±990 m^3 for both areas combined (Table 4). In the Honokowai cell, the 1949 to 1963 and the 1988 to 1992 periods show significant volume loss accounting for 64% of the gross volume change. The Kaanapali cell follows a similar trend for the same time periods accounting for 60% of the absolute gross volume change. By accounting for each historical volume change processes, it is estimated that historical Kona storms account for -136,900 m^3 or 62% of the gross volume change and post-storm recovery of 73,900 m^3 or 33% of the gross is attributed to accretion between these events (Figure 13). A residual loss of -10,700 m^3 or

5% of the gross is identified from the difference between the net volume change (-73,700 m^3) and the sum of the storm and recovery volume changes (+63,000 m^3). Residual loss may be partly attributed to RSLR as described above.

Table 4. Historical Net Volume Change (1949 to 1997)

Time Series	Net Volume Change (m^3)	% of Gross Volume Change	Volume Change Rate (m^3/yr)	Storm Loss 1949-1963 1988-1992	% of Gross Volume Change	% of Total Net Change
Honokowai						
1949 to 1961	-32,681	-33%	-2,723	-32,681	-33%	106%
1961 to 1963	5,241	5%	2,621			
1963 to 1975	-1,698	-2%	-142			
1975 to 1988	21,233	22%	1,633			
1988 to 1992	-30,350	-31%	-7,587	-30,350	-31%	99%
1992 to 1997	7,522	8%	1,504			
Gross Change	*98,725*	100%	-	**-63,031**	**-64%**	**205%**
Net Change	*-30,733*	-31%	*-640*			
Kaanapali						
1949 to 1961	-3,478	-3%	-290			
1961 to 1963	-25,812	-21%	-12,906	-29,290	-24%	68%
1963 to 1975	22,561	18%	1,880			
1975 to 1988	-8,983	-7%	-691			
1988 to 1992	-44,647	-36%	-11,162	-44,647	-36%	104%
1992 to 1997	17,360	14%	3,472			
Gross Change	*122,841*	100%	-	**-73,936**	**-60%**	**172%**
Net Change	*-42,999*	-35%	*-896*			
Total Net Sum	**-73,732**	**-33%**	**-1,536**	-136,967	-62%	186%
Storm Events	***-136,967***	**62%**				
Accretion Events	**73,917**	**33%**				
Residual Loss	-10,682	**5%**				
Total Gross	***221,566***	**100%**				

We also see that the net volume change for both cells (73,732 ±992 m^3) accounts for only roughly 30% of the absolute gross change for both cells (221,566 m^3), reflecting the dynamic nature of this area. Both cells exhibit patterns of net erosion in the early 1960's and 1990's followed by periods of recovery. An increase in short-period southerly waves during these periods is well documented by Moberly and Chamberlain, (1964) and may have transported beach sediment further offshore than normal (beyond the reef) and is identified as a possible mechanism for long-term erosion in this area.

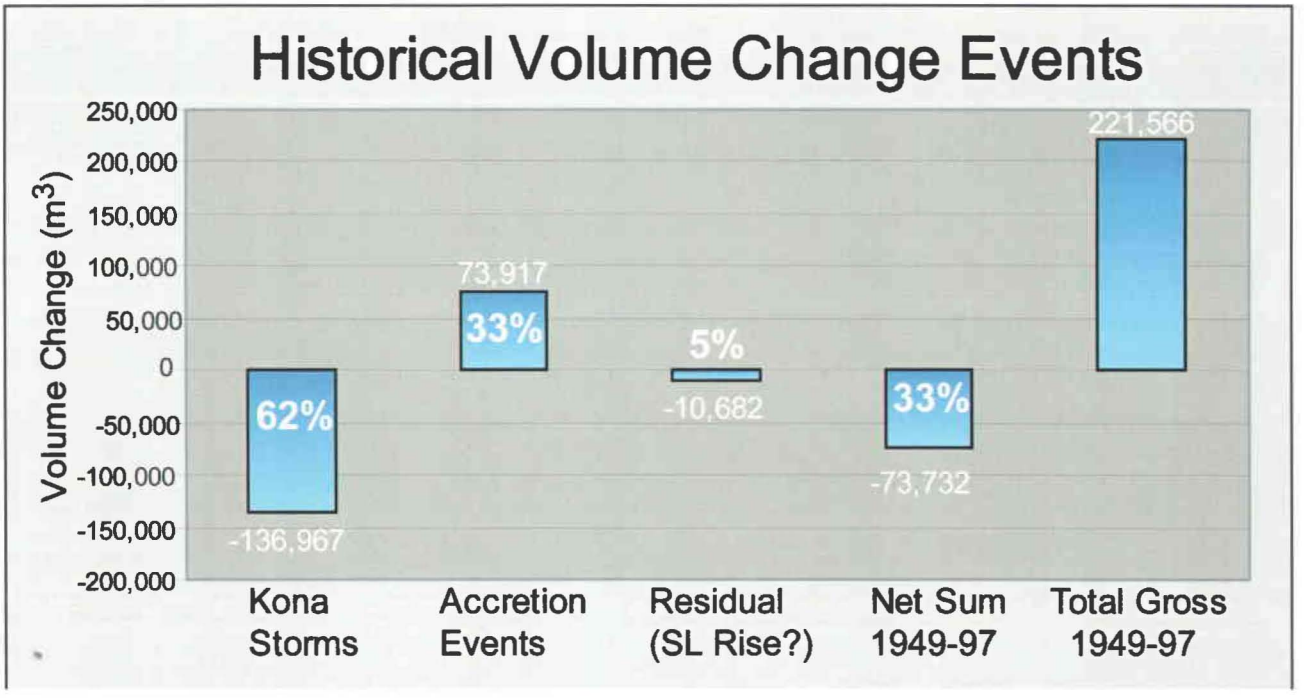

Figure 13. Historical volume change processes with percent of the gross volume change given. Quantifying the volume lost during storms and recovery after, a residual loss is calculated from the remaining difference to the total net volume.

Historical beach volume results identify pronounced net volume loss of 136,967 m^3 in the early 1960's and in 1992. This volume loss is partly attributed to increased tropical cyclone activity in the Central Pacific in the late 1950's and early 1960's (Shaw, 1981) and Hurricane Iniki in 1992. Relative sea-level rise (RSLR) of approximately 2.46 ± .23 cm/decade for Kahului Harbor, Maui (Fletcher, 2002), may be a contributing factor to the long-term (century) chronic erosion of Kaanapali but is likely overshadowed by the dominant short-term (decadal) sediment budget fluctuations.

Short-term variations in sediment delivery accounts for mean gross fluctuations on the order of 4500 m^3/yr or a total gross change of 221,500 ±1100 m^3 as opposed to the long-term residual loss of approximately 10,700 ±990 m^3 over 48yrs. Integrating the net volume change of 73,700 m^3 over the 48 year period produces an annual net loss of 1535 m^3/yr. Applying the annual net loss to the 1997 total beach volume of 432,700 ±1100 m^3, an estimated 282 years is calculated for the expected time to achieve total beach loss. It is possible to apply the RSLR at Kahului Harbor to gain a subsequent RSLR of approximately 0.69 m over the 282 year time period.

Assuming all existing environmental factors such as; RSLR, sediment availability and nearshore structures remain constant, it is possible to speculate there may be a RSLR of approximately 0.69 m over the next 282 years, in which time the current beach volume may be lost. Assuming the current local RSLR has remained constant for the last several hundred years, we would expect the beach to have migrated landward and/or eroded during this time due to the inundation of the coastal plain. Alternatively, it is also possible the beach at Kaanapali may have been roughly twice as wide during the last 300 years and has eroded to its' current width. The accretionary foreland geomorphic feature

of Kaanapali suggests a net positive supply of sediment has been in place over the long-term. While local influences on the shoreline position such as RSLR may have changed over time, it appears the relative beach width in Kaanapali has likely remained stable because of its' ability to migrate in response to the RSLR input.

Comparing net volume change to cumulative change we see an overall erosional trend for the historical time period (Figure 14). While net volume change is a good indicator of the independent change in sediment volume for each time period (Figure 14a.), cumulative sediment volume is a better gauge of the overall long-term condition of the beach and accounts for the antecedent condition of the shoreline (Figure 14b). We observe that the accretionary events from 1963 to 1988 are not sufficient to allow full recovery of the sediment volume from the previous erosion period. Likewise, if we disregard the erosional event of 1992 we might expect to see complete recovery of sediment volume suggesting the recovery time may be on the order of roughly 25 to 30 years (Figure 14c.). This implies the 1992 time period significantly destabilized the near shore beach system and played a significant role in the interpretation of the long-term erosion history of this area.

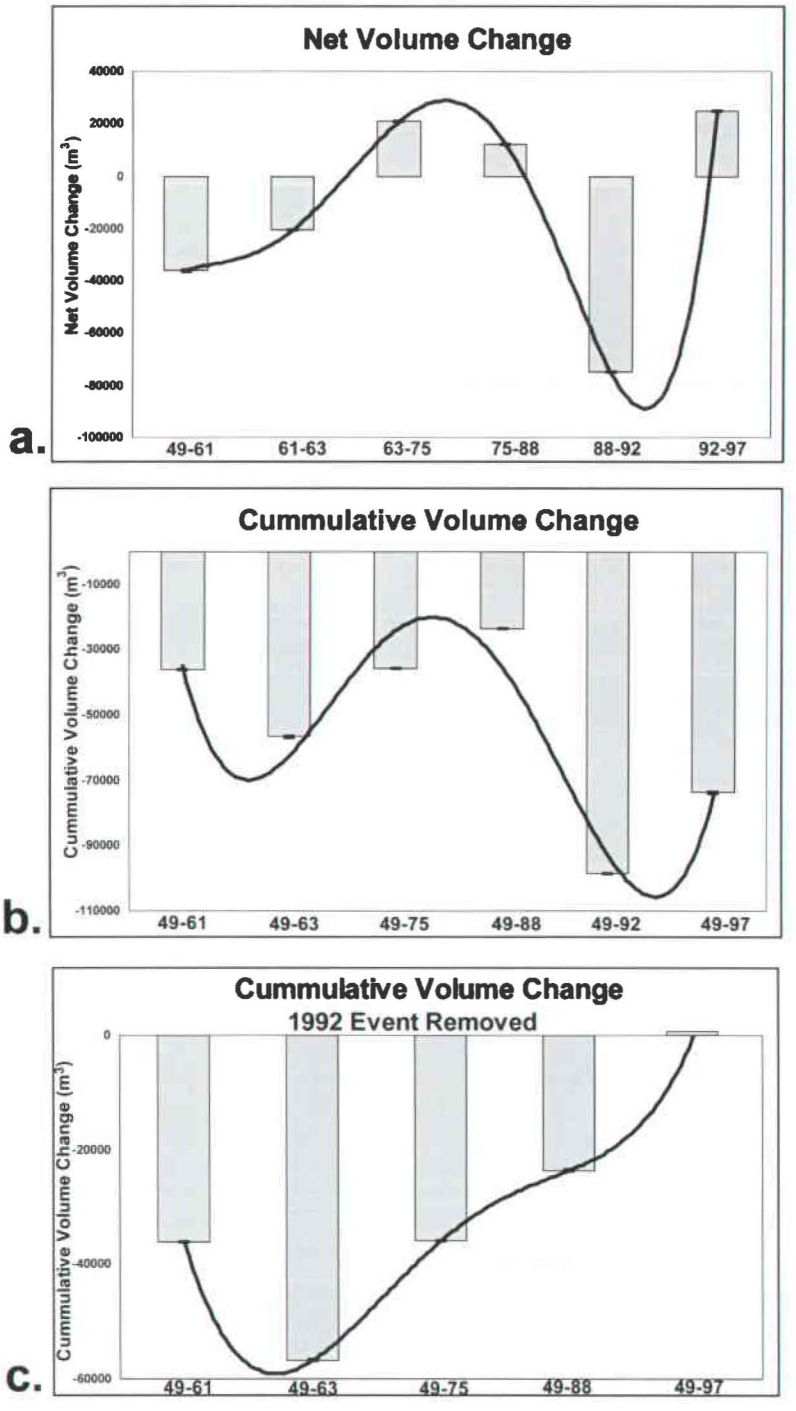

Figure 14. Net and cumulative sediment volume for Kaanapali and Honokowai cells. Note continuous erosional trend throughout time period for cumulative volume (b). Complete volume recovery is observed if the 1992 event is removed revealing its' significance in the volume history (c). Black trend line is polynomial best-fit of data.

Spatial analysis of historical volume suggests the net volume changes described above are a reflection of pronounced transport at two distinct locations along the coast. Peak fluctuation of the shoreline are found at Honokowai Point and either side of Kekaa Point, which agrees with our monthly beach survey observations. The distribution of the historic volume change clearly indicates increased volume flux at the central and south portion of the study area, near Kekaa Point and Hanakoo Point and significantly less volume change at the northern and southern ends of the study area (Figure 15).

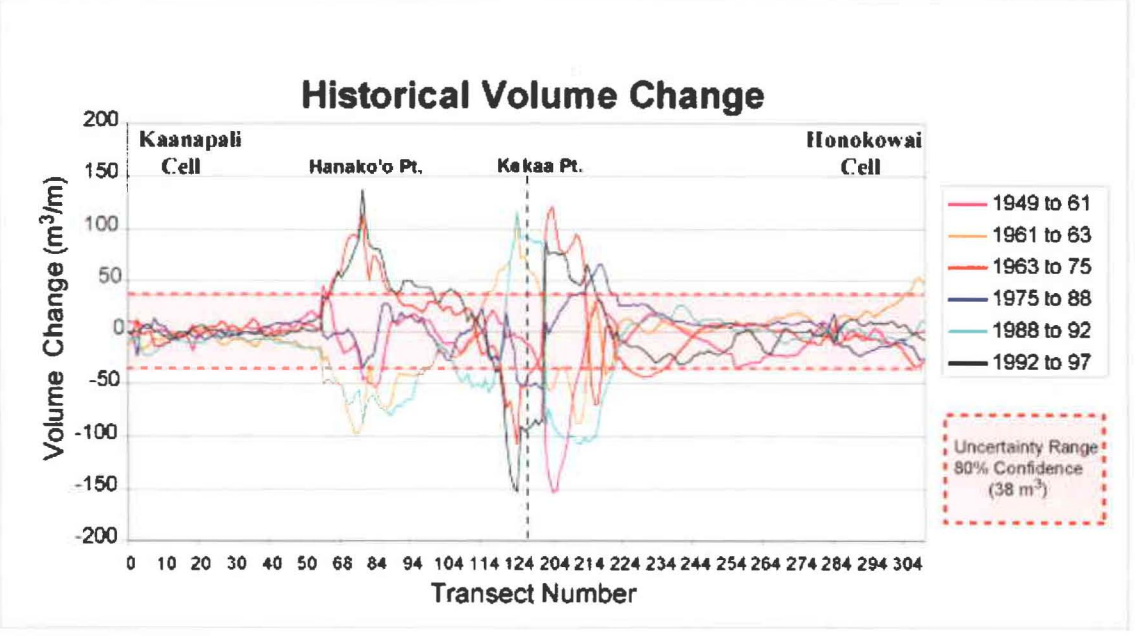

Figure 15. Spatial distribution of historic volume change. Note peak volume flux at Hanakoo and Kekaa Point.

The spatial and temporal distribution of volume change is examined using a 3-dimensional plot of the volume change rates and the cyclic nature of punctuated erosion followed by recovery for the early 1960's and 1992 is again observed (Figure 16). Along the horizontal axis of this plot we see a sequential time series of beach volume change starting at 1949 on the left and ending with 1997 on the right. The vertical axis represents the transect location along the shore and corresponds to the adjoining photomap on Figure 16. Beach volume change rates ($m^3/m/yr$) are depicted by shaded color, with red indicating erosion and blue indicating accretion from the mean for each transect. Here, increased beach volume flux is observed near Kekaa and Hanakoo Point, supporting the spatial results of Figure 16. The significant erosional effects of the early 1960's and 1992 are illustrated here again, particularly at Kekaa and Honokowai Point.

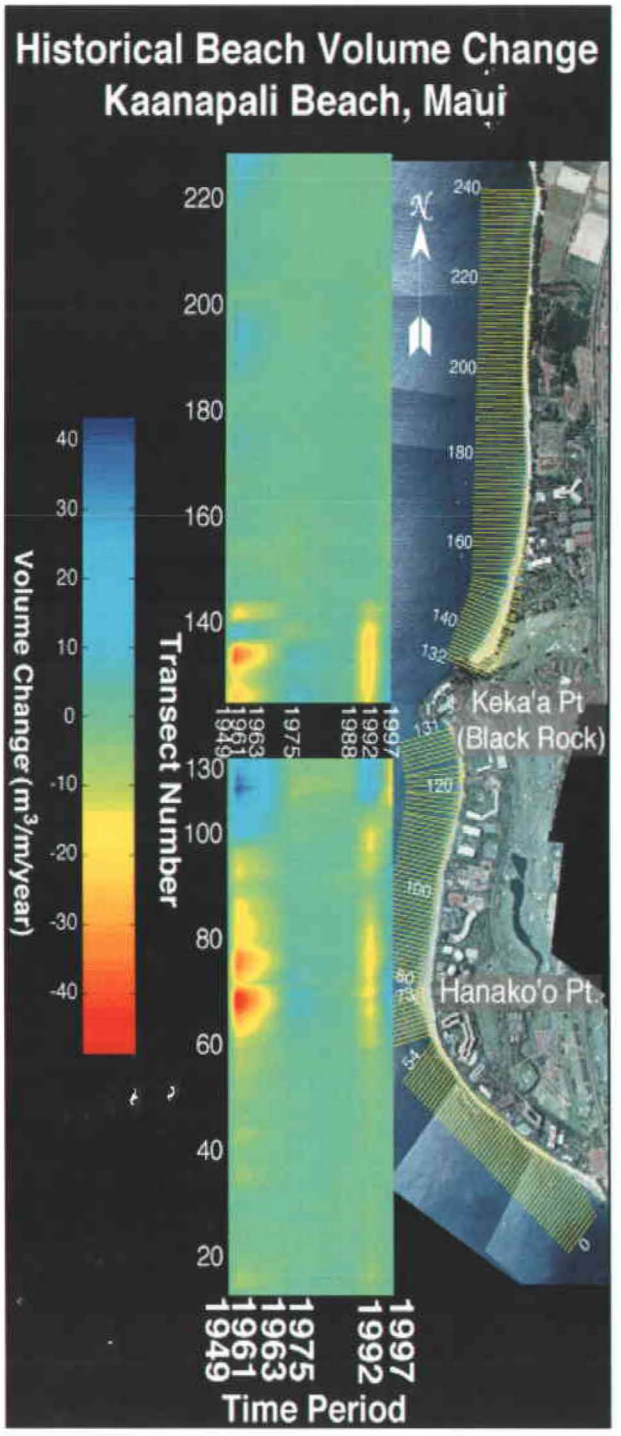

Figure 16. Distribution and magnitude of historic volume change rates.

5.2.2 Shoreline Uncertainty Analysis

Three main sources of error in are identified in the error analysis of the historical shoreline. Where: Total Position Uncertainty (*TPU*)

$$TPU = \sqrt{(\text{Measurement Error})^2 + (\text{Tidal Error})^2 + (\text{Seasonal Error})^2} \quad \textbf{(3)}$$

Measurement error is an additive error defined as the square root of the sum of squares of the photo rectification error (using student T-Test), digitizing error, toe identification error and pixel accuracy (0.5 m). Tidal error is the maximum horizontal movement of the beach toe measured between the highest and lowest tides of the spring tide. Seasonal fluctuations are by far the largest source of error and are calculated from the beach profile surveys using a student T-Test.

Horizontal seasonal uncertainty for the Kaanapali area is estimated to be ±8.8 m, which gives the Total Position Uncertainty (*TPU*) ±10.0 m at the 80% confidence interval and a total volume uncertainty for each transect of ± 27.1 m^3. This means the true value of the shoreline position lies within ±10.0 m of the estimated position with 80% confidence. Uncertainty for each dv/dx slope is calculated using the standard error of the slope from the residual values and the median slope error volume is calculated as ± 4.54 m^3 (Moore, 1993). Volume uncertainty is calculated by multiplying the *TPU* by the mean dv/dx slope for the study area (2.709). Because each of the TPU components is considered random and uncorrelated each subsequent function applied to the volume data (ie, summing net volume) requires the uncertainty be carried through as an additive error defined as the square root of the sum of squares of each uncertainty, thus our total volume change uncertainty for each time series is:

$\sqrt{(\text{Transect Uncert}_1)^2 + (\text{Transect Uncert}_2)^2}$ for all transects (Table 5). Volume

uncertainty for the sum of 6 historical time periods is calculated as ± 992 m^3 and is negligible in comparison to the historical volume changes on the order of thousands of m^3 as detailed in section 5.2.1.

Table 5. Historical Shoreline Uncertainty

Uncertainty Type	***80 % Uncertainty***
Seasonal Error (m)	± 8.8
Mean Measurement Error (m)	± 3.2
Tidal (m)	± 3
Horizontal (*TPU*) (m)	10.0
Median dV/dX slope (2.7)	± 0.45
Slope Uncertainty (m^3) (Error * TPU)	± 4.54
Volume (m^3/m) Each Transect	31.7
Volume (m^3/m) All Transects (222)	496
Volume (m^3/m) Historical Shoreline Difference	701
Volume (m^3/m) Net Shoreline Sum	992

5.3 Beach Morphology and Wave Forcing

As described in section 4.3, the filtered daily coastal wave energy is utilized for seasonal comparison to beach volume. A strong correlation between seasonal wave forcing and total volume change is observed. Total beach volume for all profiles exhibit pronounced seasonal change with both the Honokowai and Kaanapali littoral cells exhibiting clearly defined seasonal patterns in unison. Therefore, total beach volume is used for comparative analysis to wave energy. This pattern is attributed to the seasonal change in incident wave energy direction. During the summer months, southern hemisphere swells produce wave energy directed from south to north establishing a strong northward longshore transport pattern. In the winter the pattern reverses with north swells directing sediment transport to the south. There appears to be less transport of sediment south of Hanakoo Point, and north of profile 4. This may be due to the

presence of a shallow fringing reef in these areas inhibiting wave-induced sediment transport across the reef.

Incident wave energy flux is given by $F_b = \frac{\rho g^2 T H^2}{16}$ (CEM, 2001) where T and H are breaker height and period. F_b is used to compare the seasonal incident wave energy to the total monthly beach volume change from the mean (Figure 17). There is a strong correlation of the beach volume to the incident wave energy monthly mean. In general, south swells tend to decrease the total beach volume while north swells tend to increase volume. Due to the swell window, frequency and swell approach angle and its interaction with the fringing reef, south swells tend to generate more energy in Kaanapali than do north swells as exhibited in the monthly mean of the wave energy flux. The decrease in total beach volume during the summer months may be at least partly due to increased wave energy and bottom currents agitating bottom sediment and inducing offshore transport of sediment through the reef channels in the Kaanapali cell. Swell energy and direction play an important part in the seasonal dynamics of the shoreline and are the dominant forces acting on short-term (seasonal) shoreline change as observed in the cyclic pattern of balanced sediment exchange between profiles 5 and 9.

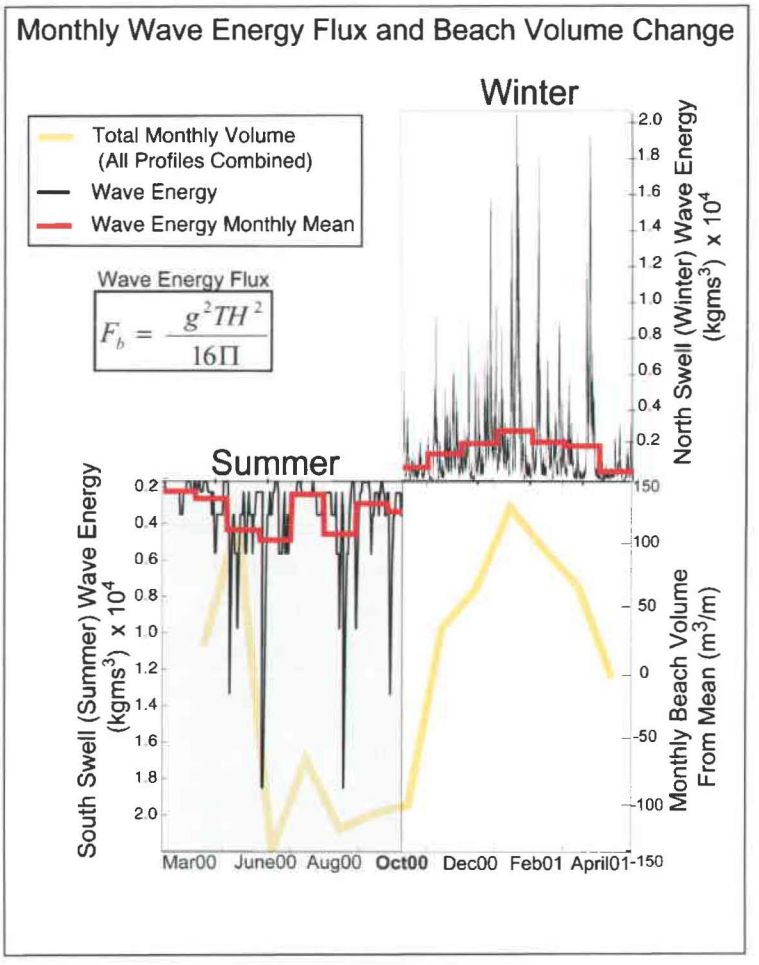

Figure 17. Filtered wave energy flux and total monthly beach volume. Monthly wave energy flux (red) and total beach volume from the mean (yellow). An increase in south swell energy (shaded summer period, March to October) corresponds to significant decrease in total beach volume in summer while the winter corresponds to volume recovery.

5.4 Statistical Cross Correlation

A statistical cross correlation technique is employed to examine lag correlations of the different profile volumes. Each profile's monthly volume is cross correlated with each other and plotted to over a 12 month period. Profiles that correlate well at or near the 0 phase shift indicate they correlate at the same time rather than at different lag intervals. Each plot reveals a lag or temporal phase shift indicated on the x -axis at which

the profiles fall in and out of correlation (Figure 18). This pattern reflects the cyclic nature of how each profile responds to one another temporally with the given r-value indicating how well they correlate. There is statistically significant correlation between profiles (1 & 2), (3 & 4), (7 & 8), (7 & 10) and (8 & 10) with r-values of (+0.80, -0.82, -0.80, -0.80, and +0.82) respectively. Negatively correlated profiles act opposite to each other, while positively correlated profiles act in unison. Positively correlated profiles may be experiencing similar wave energy exposure or sediment fluctuations that induce a similar response in profile volume at the same time. Statistical correlations match well with our seasonal profile volume observations and suggest profile volume changes are a result of wave-induced longshore sediment transport.

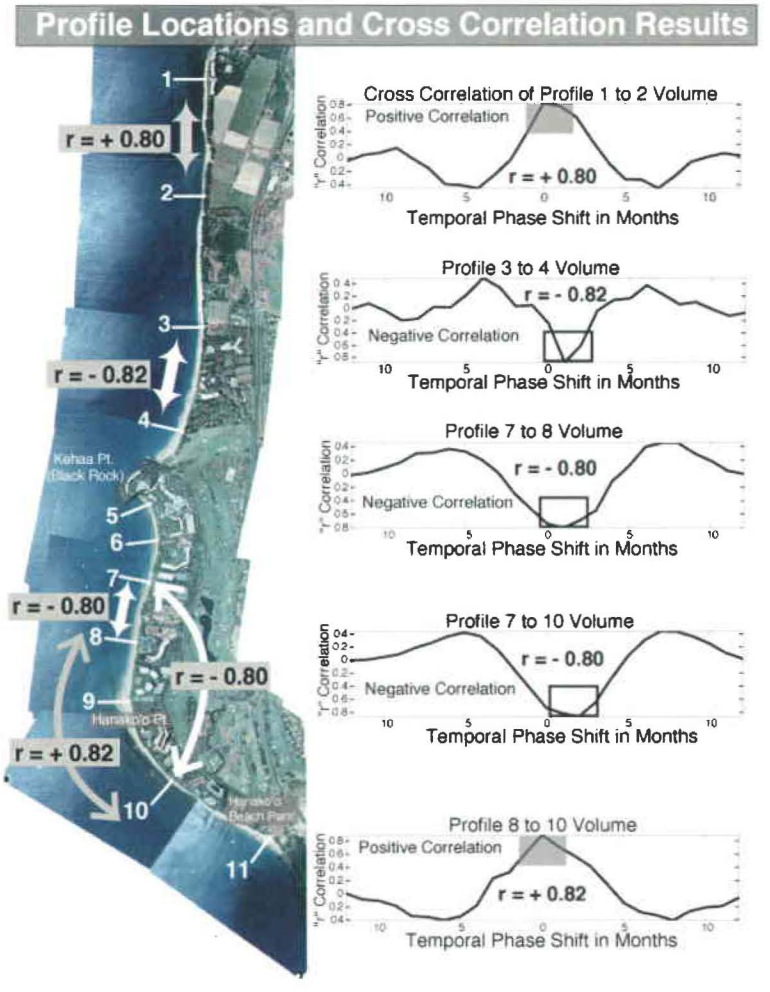

Figure 18. Cross correlation statistical results. Arrows indicate the profiles that are correlated. Negative r-values imply the profiles act opposite each other, positive r-values (gray shading) imply profiles act in unison.

5.5 EOF Analysis

Empirical Orthogonal Functions (EOF) were applied to historical beach width and monthly profile data sets. Using EOFs, the dominant modes of variability for the historical beach widths and profiles are examined both temporally and spatially. Together modes 1 and 2 account for 90% of the profile variability and 73% of the photo variability revealing most of the change falls into these dominant patterns. 79% and 44% of the profile and historical photo variability respectively can be attributed to mode 1 variability. Increased variability at Hanakoo and Kekaa Point is identified using EOFs for spatial analysis of beach width in modern beach profiles and historical photographs. The spatial behavior of these modes supports the model of shoreline instability at Hanakoo and Kekaa Points (Figure 19).

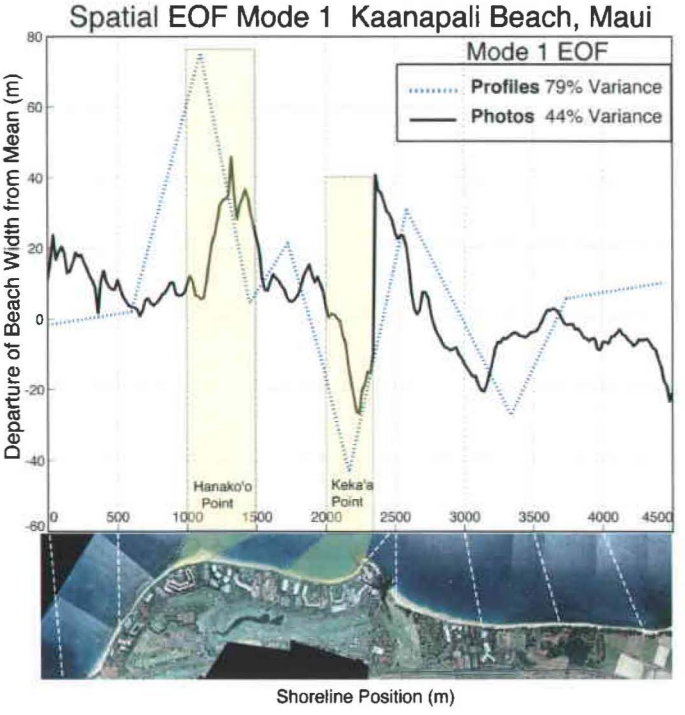

Figure 19. Spatial EOF (mode 1) for profiles and historical beach widths. Note increased variability at Hanakoo and Kekaa Point.

Using EOFs to investigate the temporal distribution of historical beach width highlights the significance of seasonal beach width change. Two distinct periods of beach width loss are identified in 1963 and 1992. The seasonal state at the time each photo was taken is also given (Figure 20). All the photos taken in winter months imply a beach width increase while the two summer photos illustrate significant erosion, suggesting seasonal uncertainty may partially influence the interpretation of historical shoreline behavior. However the seasonal total position uncertainty and thus sediment volume uncertainty (section 5.6) are unable to account for the large-scale historical volume changes observed. While the mode 1 analysis may identify some of the seasonal flux within each photo, mode 2 likely better illustrates the trend of the shoreline with the seasonal flux removed. The trend of the mode 2 plot reveals a net loss of beach width and supports the model of a shoreline that has ultimately lost beach width over the time period.

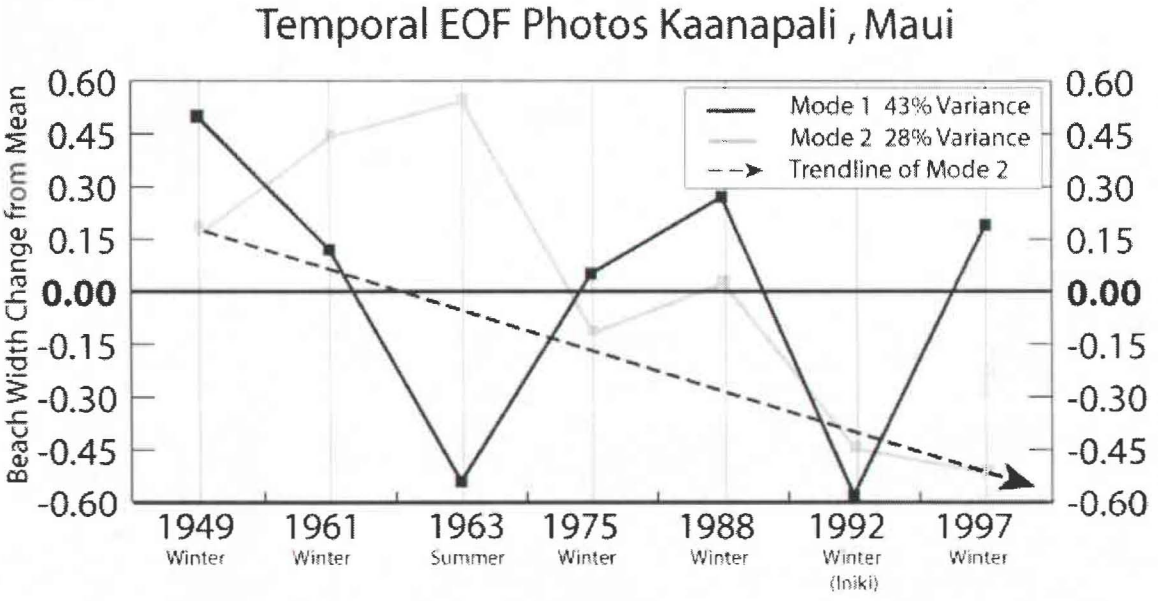

Figure 20. Temporal EOF for historical beach widths. Unitless EOF analysis of beach width change reveals punctuated erosion in 1963 and 1992. The seasonal state of each photo implies some seasonal influence however the trend of the mode 2 plot likely better represents the long-term trend of beach erosion as indicated by the dashed line.

5.6 Longshore Sediment Transport

Longshore Sediment Transport (LST) is of great significance to the seasonal and long-term dynamics of the Kaanapali coastline. Analysis of monthly profile volume, on-site and offshore observations of seasonal wave forcing and statistical cross-correlation of beach profiles (Sections 4.1.1 and 5.3 to 5.4) suggest profile volume change in the Kaanapali area is dominated by longshore transport. Beach profile results indicate sediment impoundment occurs seasonally and exhibits a nearly balanced longshore-net sediment flux between profile 5 and 9 implying the profile volume change is controlled by longshore transport (Table 6). Accretion of sediment is attributed to impoundment at Kekaa and Hanakoo Point due to longshore transport by wave forcing. Observed estimates of longshore transport from our profile data are compared to 3 commonly used predictive LST models: CERC, (1984), CERC, (1991) and Kamphius, (1991).

Table 6. Observed Net Profile Volume Change

Observed Profiles	Net Volume Change ($m^3/m/yr$)			
Kaanapali		**Profile 9**	**Profile 5**	**Percent Change**
	Net Summer Change	-138	147	107%
	Net Winter Change	77	-76	99%
	Annual Gross Change	315	306	97%
	Annual Net Change	-61	71	116%

Table 6. Observed net sediment volume change. Note the balanced seasonal longshore transport of sediment between profile 9 and 5.

Cumulative longshore beach volume is calculated based on beach profile sectional volumes (profile volume per unit of beach). Sectional volumes are in turn multiplied by longshore distance between each profile (250 m) to account for monthly volume change for each section of beach. In order to integrate over the entire area and reduce effects of seasonal outliers, the cumulative net sum longshore is calculated as a proxy for longshore transport rates (Figure 21). In order to insure accurate comparison of volume changes we evaluate the cumulative volume at profile 7 (volume cell 3) for the observed transport and compare this to the LST models.

Profile 7 was selected as a common location for comparative analysis and exhibits an inflection or hinge point in the trend of the data (Figure 22). We also find the Genesis prediction closely approximates (77%) of the observed net annual transport at profile 7.

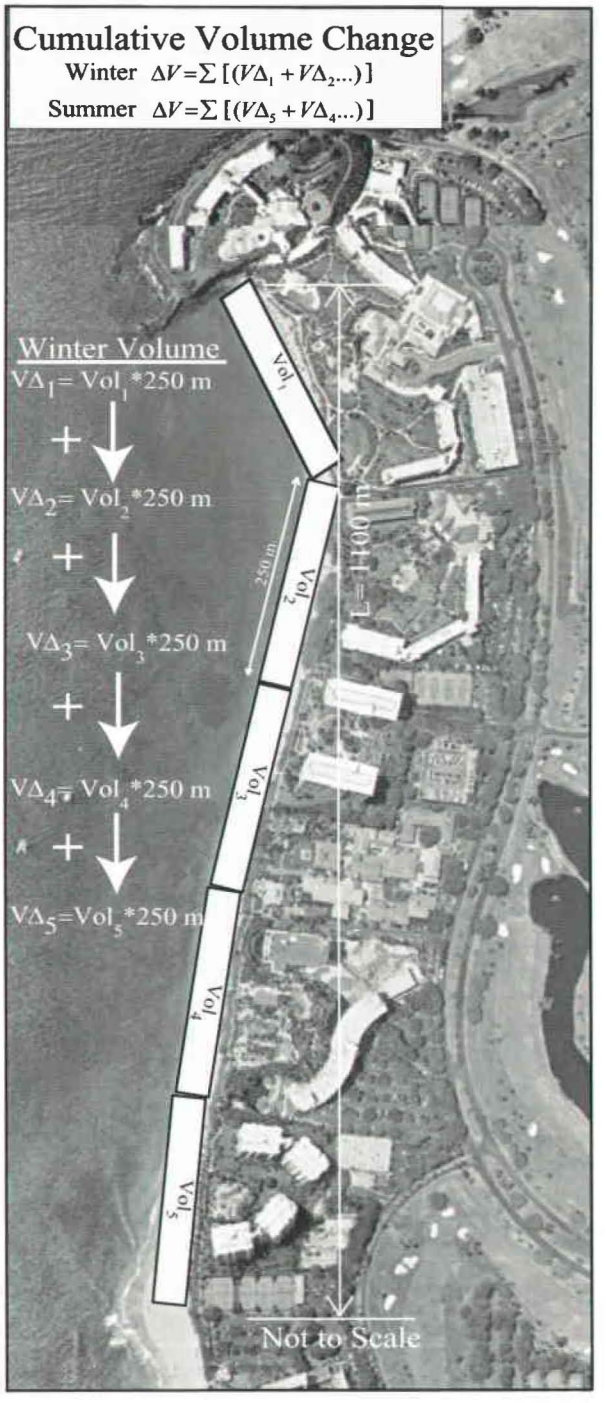

Figure 21. Cumulative profile volume change. Cumulative longshore volume change derived from profile volumes. Winter cumulative volume change calculated from profile vol_1 to vol_5, while summer is calculated from vol_5 to vol_1.

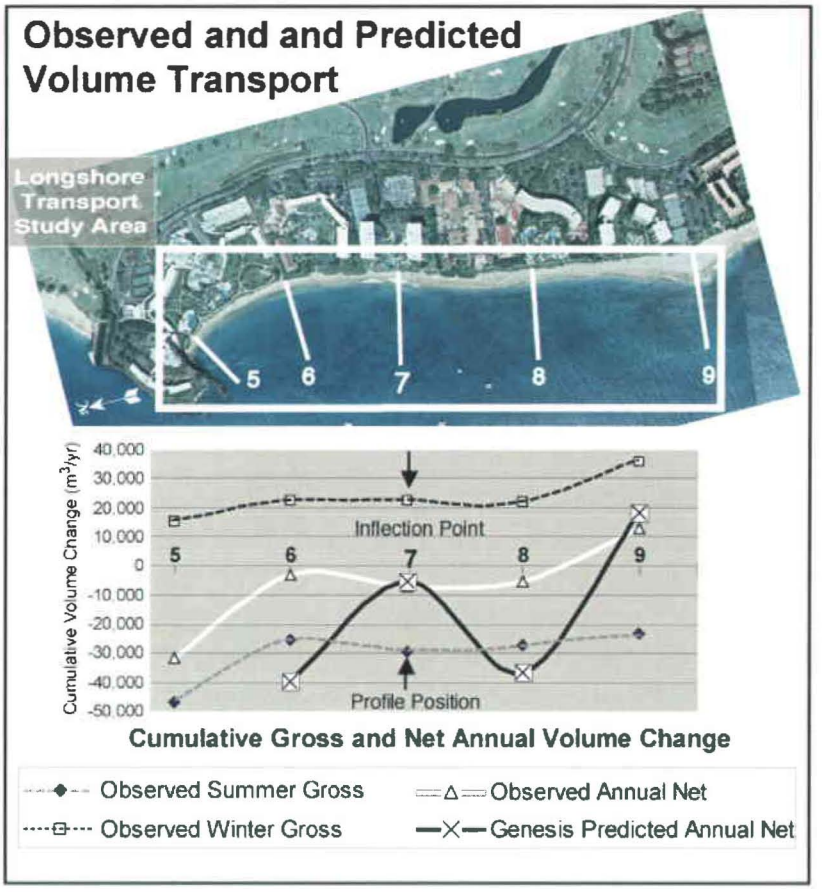

Figure 22. Cumulative seasonal gross and annual net volume change. Cumulative longshore volume change derived from profile volumes (observed) and Genesis model (CERC, 1991). Note common seasonal inflection point at profile 7 and the coincidence of the net annual transport for the observed and Genesis. Photo map is May, 1997.

Total longshore transport rates measured by Ping Wang *et al.* (1998) suggest the CERC, (1984) model predicts rates unrealistically high for low energy settings. Ping Wang *et al.* (2002) further tested the application of the Kamphius, (1991) model in a wave tank and found significantly greater LST rates under plunging breakers than spilling breakers with similar height, implying wave period significantly alters the LST rates for the Kamphius, (1991) model. Similarly, we find that the predicted CERC (1984, 1991)

and Kamphius, (1991) modeled LST rates for Kaanapali are most sensitive to wave direction and height and both formulas closely follow wave energy non-linearly.

Table 7. Observed Volume Change and Predicted TLST rates (Negative indicates northward transport)

Observed Profiles	Volume Change	Transport Volume (m^3/yr)	Uncertainty
Kaanapali	Cumulative Gross Summer Transport	-29,379	±15%
Cumulative Volume	Cumulative Gross Winter Transport	22,358	±15%
Change at Profile 7	Net Annual TLST	**-7,021**	±6%
	Total Beach Volume	*432,731*	
Modeled TLST	**CERC, 1991 Genesis Model**	**Transport (m^3/yr)**	**% of Observed**
Predicted	Cumulative Gross Summer Transport	-22,955	78%
Cumulative Volume	Cumulative Gross Winter Transport	17,558	79%
Change at Profile 7	Net Annual TLST	**-5,397**	77%
	CERC, 1984 Model		
	Gross Summer Transport	-446,651	1520%
	Gross Winter Transport	189,288	847%
	Net Annual TLST	**-257,363**	3665%
	Kamphius, 1991 Model		
	Gross Summer Transport	-895,022	3046%
	Gross Winter Transport	427,210	1911%
	Net Annual TLST	**-467,813**	6663%

LST rates are estimated from monthly profile data and compared to three predictive transport models (Table 7). The observed cumulative net annual profile volume change at profile 7 is applied as a proxy of the LST rate. Estimated LST rates from beach profiles are compared to the CERC, (1984, 1991) and Kamphius, (1991) predictions. The CERC, (1984) and Kamphius, (1991) models over-predict the LST rates of the observed cumulative net rates while the CERC, (1991) model slightly underestimates our observed transport. Although the predicted magnitude varies widely, all three models utilized agree on the seasonal gross and annual net LST direction. We

density of these formulas in finer, well-sorted silica beaches which may account for a small portion of the over prediction.

The fringing reef plays a role in the accuracy of these LST models as well. The fossil coral reef present restricts the sub aqueous beach profile area actively involved in sediment transport and truncates the surface area of the beach profile, reducing the total area that is available for sediment exchange. This effectively produces less sediment available for transport than expected from a full-sand profile beach system that the LST models are calibrated for. However the fact that the CERC, (1984) model underestimates the observed transport implies that additional environmental parameters play a more substantial role than the influence of the reef in the model results.

LST models are very sensitive to incident wave angle and height thus detailed wave modeling or field measurements are essential for accurate results. Larger incident wave angles produce larger transport rates in observations and models. Wave modeling carried out in the *Genesis* model CERC, (1991) for Kaanapali yields a mean summer incident swell angle from the south of 7.1° from shore-normal, and a mean winter incident swell angle from the north of 3.5°. The approach angle has a direct influence on the direction and magnitude of the LST rate and is one of the primary influences of seasonal transport of sediment in the study area.

The large difference in each LST model's result can be attributed to their ability to accurately assess wave energy. The success of the *Genesis* model is attributed to its' ability to account for wave energy flux for individual events rather than a time-averaged mean as applied to the CERC, (1984) and Kamphius, (1991) formulas. The Kamphius, (1991) model utilizes several input parameters that the CERC, (1984) model does not

(Table 8). The *Genesis* model employs the most input parameters including near-shore parameters such as antecedent beach conditions, bathymetry, wave shoaling, diffraction, and several shore face parameters not accounted for in the CERC (1984) or Kamphius (1991) formulas. Overestimates of longshore transport using the CERC (1984) and Kamphius (1991) models may be partly attributed to the use of time-averaged seasonal significant wave height, period and direction as input parameters where as the CERC (1991) model utilizes an internal wave model that accounts for each wave event and considers the antecedent conditions of the shoreline.

Table 8. LST Model Input Parameters

Input Parameters	**Models**		
	Genesis	***Kamphius 91***	***CERC 84***
Wave Period	X	X	
Wave Height	X	X	X
Wave Direction	X	X	X
Bathymetry	X		
Wave Shoaling and Refraction	X		
Antecedent Conditions	X		
Beach Slope		X	
Sediment Grain Size	X	X	
Berm Height	X		
Depth of Closure	X		
Shoreline Position	X		
Alongshore Cell spacing	X		
Gravitational Constant	X		X
Water Density	X		X
Finite Time Series	X		
Empirical K-Coefficient	X		X

Although the CERC, (1984) and Kamphius, (1991) formulas overestimate the observed transport by an order of magnitude they are still useful as a qualitative interpretive tool of the transport direction. Problems with the practical application of these formulas such as improper adjustment of the *K* coefficient of proportionality used

in the CERC, (1984) model is common. The Shore Protection Manual (CERC, 1977 & 1984) recommends using a K value of 0.77 which can result in significant over prediction of LST (Bodge, personal communication, 2002). It is common practice to lower the K coefficient by an order of magnitude in order to achieve reasonable results of LST. Sea Engineering, (1996) found gross sediment transport measured from sediment traps to be ~40,000 m^3/yr for West Kauai. Using the CERC, (1984) LST formula they calculated a gross annual sediment transport rate of 1,688,900 m^3/yr. Sea Engineering determined a new wave power coefficient (K) by reducing this value by an order of magnitude and calculated a new gross annual transport rate of 269,880 m^3/yr, which fits the observations better.

Similar results are found in this study for the CERC, (1984) formula with LST estimates approximately an order of magnitude higher that observed. By using a new K value of 0.07 instead of the CERC suggested 0.7 a much better fit to the observed LST is found (Table 9). The CERC (1984) and Kamphius, (1991) formulas appear to overestimate wave energy thus when the wave energy is reduced by ½, net transport rates are reduced by an order of magnitude approximating 115% and 415% respectively of the observed values.

Table 9. Predicted TLST Rates for CERC (1984) with K=0.07 (Negative indicates northward transport)

Modeled TLST	CERC, 1984 Model (K= 0.07)	Transport (m^3/yr)	% of Observed	% Improvement
Predicted	Gross Summer Transport	-40,605	177%	1343%
Cumulative Volume	Gross Winter Transport	18,338	104%	742%
Change at Profile 7	Net Annual TLST	-22,266	413%	3253%

Table 9. Predicted LST rates for adjusted CERC, (1984) with K=0.07. With a modified empirical coefficient (K=0.07 instead of K= 0.77) we see the better fit of the predicted transport to the observed transport.

In using the LST models and formulas, it is important to recognize each model's strength and weakness and utilize the formulas collectively as an interpretive tool rather than an absolute gauge of LST. Each model should be used in conjunction with at least one other formula in order to confirm the gross and net transport direction and secondly as a rough estimate of LST magnitude. This method works very well for this study and yields consistent results on the direction of transport. All the models employed agree on the direction of seasonal gross and net annual LST even though they vary widely on the magnitude.

The presence of fringing reef also controls the incident wave energy and sediment transport capacity as well as providing a source of nearshore sediment. Based on the estimated modern sediment production of the nearshore fringing reefs, reef-supplied sediment is insignificant in comparison to the magnitude of seasonal sediment volume changes observed. Sources and sinks of sediment such as streams and offshore losses are unquantified in this study and are estimated to represent less than 5% of the gross beach sediment change. The LST models employed in this study do not account for the presence of reef, which is described in Section 2 and 5.1.3. This may partly contribute to the general over-estimate of transport in Kaanapali.

5.7 Near-shore Reef Influence

The orientation of the fringing reef plays a significant role in the stability of the beach in this area (Inman and Waldorf, 1978) (Figure 24). Mean beach volumes, beach volume range and historical volume change rates are significantly lower adjacent to fringing reefs, implying the reefs stabilize the beach. Landward of the fringing reefs, the beach is subject to less direct wave exposure due to wave energy decay over the reef flat. The reduced wave energy (adjacent to the fringing reefs) appears to decrease sediment transport. Munoz-Perez, *et al.*, (1999) investigate the distribution of reef protected beaches in Spain and conclude reef protected beaches tend to have steeper slopes and tend not to reach an equilibrium profile 10 to 30 H_r from the landward edge of the reef, where H_r is water depth over the reef. Similar results for segments of Kaanapali are recognized where a shallow (<1 m deep) reef extends to the toe of the beach at profiles 1, 2, 3, and 10. Beach profiles landward of these fringing reefs exhibit narrower but more stable characteristics that the non-reef protected profiles, suggesting the reef may inhibit a true beach equilibrium profile.

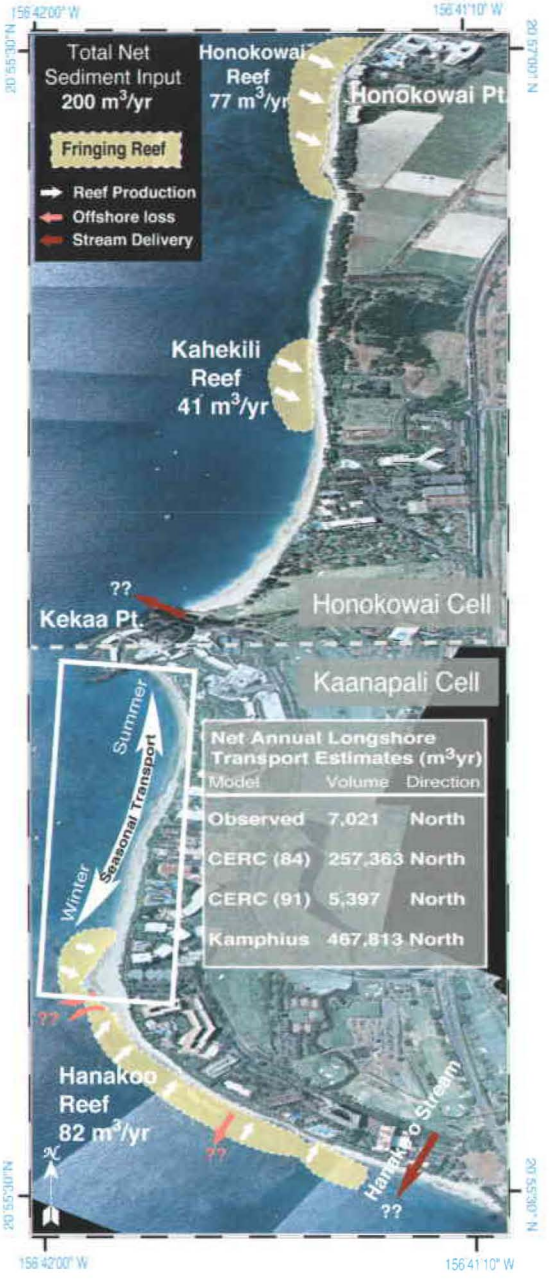

Figure 24. Sediment transport conceptual model and reef-derived sediment volumes.

6.0 CONCLUSIONS

Incorporating modern beach profile behavior with historical beach widths from orthorectified aerial photos, a quantitative record of historical shoreline volume change for the Kaanapali area is established using a volumetric change model. Historical erosion and accretion patterns reveal the Kaanapali area is subject to long periods of mild accretion punctuated by severe erosional events related to short-period Kona storms and hurricane waves. The early 1960's and 1992 are identified as significant erosional periods. Increased Central Pacific tropical cyclone activity of the late 1950's and early 1960's and Hurricane Iniki in 1992 are identified as contributing factors to the observed volume change during these periods. Between these erosional periods the Kaanapali shoreline is relatively stable characterized by light erosion to moderate accretion suggesting the recovery time may be on the order of roughly 25 years.

Comparing net volume change to cumulative change, an overall erosional trend for the historical time period is observed. The accretionary events from 1963 to 1988 are not sufficient to allow full recovery of the sediment volume from the previous erosional periods. If we disregard the erosional event of 1992 we see complete recovery of sediment volume. This implies the 1992 time period significantly destabilized the near shore beach system and plays a significant role in the interpretation of the long-term erosion history of this area.

The spatial distribution of historical and modern shoreline movement is identified and suggests the majority of sediment transport occurs in the central and southern portion of Kaanapali at Kekaa and Hanakoo Points and is driven by longshore rather than cross-shore transport.

The Kaanapali and Honokowai cells have experienced a net loss of 43,000 $\pm 730 m^3$ and 30,733 $\pm 630 m^3$ respectively over the 48-year period 1949 to 1997 for a total net volume loss of 73,732 ± 990 m^3. Historical net volume uncertainty is calculated as $\pm$ 992 m^3 and is negligible in comparison to historical volume changes. Kona storms of the early 1960's and 1992 collectively account for roughly 60% of the total gross volume. Recovery after each of these storms accounts for 73,900 m^3 or approximately 33% of the gross volume change. A residual loss of 10,600 m^3 representing 5% of the gross volume change is inferred as chronic erosion and may be a product of relative sea-level rise (RSLR). An increase in short-period southwesterly wave energy during these erosional periods is well documented and may have transported beach sediment further offshore than normal (beyond the reef) and is identified as a possible mechanism for long-term erosion in this area.

Surveyed beach profiles reveal a strong seasonal variability with net erosion in the summer and net accretion in the winter. Summer erosion is at least partly due to increased wave energy and bottom current agitating bottom sediment and inducing offshore transport of sediment through the reef channels in the

Kaanapali cell. 65% of the net volume change occurs south of Kekaa Point confirming the more dynamic nature of the southern (Kaanapali Cell). Net volume change from the mean suggests that June and January are the most dynamic months each with approximately 14% of the total volume change. Observations of net seasonal sediment volume change from beach profiles reveals there is balanced seasonal sediment exchange between profiles 5 and 9.

Longshore transport rates are derived from seasonal cumulative beach volume change in the middle of Kaanapali Beach at profile 7. Cumulative gross sediment transport rates of 29,379 ±15% m^3/yr to the north and 22,358 ±6% m^3/yr to the south for summer and winter respectively, a net annual rate of 7,021 ±10% m^3/yr to the north and a gross annual rate of 51,736 ±2% m^3/yr are observed. Predictive transport formulas such as the CERC (1984), CERC, (1991) and Kamphius, (1991) predict net annual transport rates at 3 x 10^3 percent, 77 percent and 6 x 10^3 percent of the observed transport rates respectively.

Estimated LST rates from beach profiles are compared to the predicted CERC (1984, 1991) and Kamphius, (1991) predictions. The CERC (1991) *Genesis* model best fits the observed LST rates for Kaanapali with a net annual LST rate within 77% of our observed mean gross annual rate. The CERC (1984) and Kamphius, (1991) models over-predict the LST rates of the observed cumulative net rates while the CERC (1991) model slightly underestimates our observed transport model.

Although the predicted magnitude varies widely, all the three LST models utilized agree on the seasonal gross and annual net direction. Adjustment of the empirical *K* value in the CERC, (1984) LST model to 0.07 significantly improves the fit to observed data. All LST models agree in a net northward transport in the summer, net southward transport in the winter and an annual net LST to the north.

The position and orientation of the fringing reef plays a significant role in the stability of the shoreline creating narrow steep beaches that are often significantly more seasonally stable than the surrounding non-reef beaches. The narrow but stable seasonal morphology of the reef-protected beaches is attributed to decreased onshore wave energy, decreased near shore sediment transport and sediment transport offshore through the reef channels.

The fossil coral reef that fronts Kaanapali Beach influences the results of the LST models. Shallow fringing reef truncates the subaqueous area of several of the beach profiles reducing the total volume that is available for sediment exchange. This effectively produces less sediment available for transport than expected from a full-sand profile beach system that the LST models are calibrated for. However the fact that the CERC, (1991) model underestimates the observed transport implies that additional environmental parameters (such as wave height, direction and period) play a more substantial role than the influence of the reef in the model results.

References

Armstrong, R.W., 1983. Atlas of Hawaii. University of Hawaii Press, Honolulu, p.238.

Aubrey, D.G., 1979. Seasonal Patterns of Onshore/Offshore Sediment Movement. Journal of Geophysical Research, 84. 6347-6354.

Bodge, K.R, Dean, R.G., 1987. Short-term impoundment of longshore transport. Proc Coastal Seds 1987, ASCE, p. 468-483.

Bodge, K., Kraus, N., 1991 Critical examination of longshore transport rate magnitude. Coastal Sediments Vol I, 1991. p. 139-155.

Bodge, K.R., 1998. Sediment Management at Inlets/Harbors. U.S. Army Corps of Engineers Coastal Engineering Manual (Draft) Part V, Ch.6.

CERC, 1984. Shore Protection Manual. U.S Army Corps of Engineers, Coastal Engineering Research Center. U.S. Government Printing Office, Washington. D.C.

CERC, 1991. GENESIS: Generalized Model for Simulating Shoreline Change. Technical Report CERC-89-19. U.S Army Corps of Engineers, Coastal Engineering Research Center. U.S. Government Printing Office, Washington. D.C.

CEM, 2001. Coastal Engineering Manual. U.S Army Corps of Engineers, U.S. Government Printing Office, Washington. D.C. Chapter 2. Water Wave Mechanics 1-28.

Crowell, M., Honeycut, M., Hatheway, D., 1999. Coastal Erosion Hazards Study Phase One Mapping. Journal of Coastal research, Special Issue No. 28. 10-19.

Coyne, M.A., Fletcher, C.H., Richmond, B.M., 1999. Mapping Erosion Hazard Areas in Hawaii: Observations and Errors. Journal of Coastal research, Special Issue No. 28, 171-184.

Dail, H.J., Merrifield, M.A., Bevis, M., 1999. Steep Beach Morphology Changes Due to Energetic Wave Forcing. Marine geology, 162. p. 443-458.

Dean, R.G., 1989. Measuring Longshore Sediment Transport with Traps. In: Seymour, R.J. Nearshore Sediment Transport, New York. Plenum Press, p. 313-337.

Dean, R.G., 1977. Equilibrium Beach Profiles: US Atlantic and Gulf Coasts. Ocean Engineering Report No.12, Department of Civil Engineering, University of Delaware, Newark, Delaware.

Dick, J.E., Dalrymple, R.A., 1984. Coastal Changes at Bethany Beach, Deleware. Proc. 19th Int. Conf. Coastal Engineering, ASCE. New York, NY. 1650-1667.

Fletcher, C.H., Grossman, E.E., Richmond, B.M., Gibbs, A.E., 2002. Atlas of Natural Hazards in the Hawaiian Coastal Zone. United States Geological Survey, Geological Investigations Series I-2761, p. 21.

Fletcher, C.H., Hwang, D.J., 1994. Shoreline Certification Review and Recommendations. Office of State Planning, Coastal Zone Management Program, Honolulu, p.76.

Fletcher, C.H., Mullane, R.A., Richmond, B.M., 1997. Beach Loss along armored shorelines on Oahu, Hawaiian Islands. Journal of Coastal Research, 13 (1), 209-215.

Fletcher, C.H., Lemmo, S.J., 1999. Hawaii's Emergent Coastal Erosion Management Program. Shore and Beach, 67 (4), p. 15-20.

Gerritson, F., 1978. Beach and Surf Parameters in Hawaii. University of Hawaii Sea Grant College Program. P.178.

Grigg, R.W., Jones, A.T., 1997. Uplift Caused by Lithospheric Flexure in the Hawaiian Archipelago as Revealed by Elevated Coral Deposits. Marine Geology, 141, P. 11-25.

Hallermeier, R.J., 1978. Uses for a Calculated Limit Depth to Beach Erosion. Proc.16th Coastal Eng. Conf. ASCE, New York, 1493-1512.

Harney, J.N., Grossman, E.E., Richmond, B.M., Fletcher, C.H., 1999. Age and Composition of Carbonate Shoreface Sediments, Kailua Bay, Oahu, Hawaii. Coral reefs, 19. 141-154.

Inman, D.L., Waldorf, B.W., 1978 Beach and Reef Study, South Beach Kaanapali, Maui. Report for Amfac Communities-Maui. Intersea Research Corporation, July 1978.

Juvik, S.P., Juvik, J.W., 1998 Atlas of Hawaii. University of Hawaii Press, Honolulu, p.82.

Kamphius, J.W., 1991. Longshore Sediment Transport Rate. Journal of Waterway, Port, Coastal and Ocean Engineering, ASCE, 117 (6), 624-641.

Komar, P.D., Inman, D.L. 1970. Longshore Sand Transport on beaches. Journal of geophysical research, 75 (30), 5514-5527.

Kraus, N.C., Larson, M., Kriebel, D.L. 1991. Evaluation of Beach Erosion and Accretion Predictors. Paper Presented at Coastal Sediments, Am. Soc. Civ. Eng., Vol 91, Seattle, W.A.

Makai Ocean Engineering, Inc., and Sea Engineering Inc., 1991. Aerial photographic Analysis of Coastal Erosion on the Islands of Kaui, Lanai, Maui and Hawaii. Office of Sate Planning, Coastal Zone Management Program. Honolulu, p.200.

Moberly, R., Cox, D., Chamberlain, T., McCoy, F.W., and Cambell, J.F., 1963. Coastal Geology of Hawaii. Hawaii Institute of Geophysics report No. 41, Honolulu, p.216.

Moberly, R., Chamberlain,T., 1964. Hawaiian Beach Systems. Hawaii Institute of Geophysics University of Hawaii, Final Report. Harbors Division, Department of Transportation, State of Hawaii Contract no.6496.

Moore, D, S., McCabe, G, P., 1993. Introduction to the practice of statistics. 2nd Edition. Freeman and Company, New York. p. 665.

Munoz-Perez, J.J., Tejedor, L., Median, R., 1999. Equilibrium Profile Model for Reef-Protected Beaches. Journal of Coastal Research 15 (4). p 950-957.

Norcross, Z.M., Fletcher, C.H., Merrifield, M.A., (In Press). Large-Scale Longshore Meanders on a Carbonate Beach Substitute for Seasonal Morphology in Response to Wave State.

Richmond, B.M., Fletcher, C.H., Grossman, E.E., Gibbs, A.E. 2001. Islands at Risk: Coastal Hazard Assessment and Mapping in the Hawaiian Islands. Environmental Geosciences Vol. 8 (1) p. 21-37.

Rooney, J.J., Fletcher, C.H. 2000. A High Resolution, Digital, Aerial-Photogrammetric Analysis of Historical Shoreline Change and net Sediment Transport Along the Kihei Coast of Maui, Hawaii. Proc.13th Annual National Conference Beach Preservation Technology. February 2-4, 2000, Melbourne, Florida.

Sea Engineering, Inc., 1988. Oahu Shoreline Study. City and County of Honolulu, Dept of land Utilization, Honolulu, p.126.

Sea Engineering, Inc., 1996. Sediment Transport at Kikiaola Harbor, Island of Kauai, Hawaii. Prepared for: U.S. Army Engineering Division, Pacific Ocean, Fort Shafter, Hawaii. August, 1996.

Wang, P., Smith, E.R., Ebersole, B.A., 2002. Large-scale Laboratory Measurements of Longshore Sediment transport Under Spilling and Plunging Breakers. Journal of Coastal Research 18 (1). p 118-135.

Shaw, S.L., 1981. A History of Tropical Cyclones in the Central North Pacific and the Hawaiian Islands 1832-1979. U.S. Dept of Commerce, National Oceanic and Atmospheric Administration, National Weather Service Report September, 1981.

Short, A.D., 1999. Handbook of Beach and Shoreface Morphodynamics. John Wiley and Sons, Inc., New York p. 177

Smith, G.L., Zarillo, G.A., 1990. Calculating Long-term Shoreline Recession rates Using Aerial Photographic and Beach Profiling techniques. Journal of Coastal Research, 6 (1). p 111-120.

Thieler, R.E., Danforth, W.W., 1994. Historical Shoreline Mapping (I): Improving techniques and Reducing Positioning Errors. Journal of Coastal research, 10 (3). 549-563.

Wang, P., Kraus, N.C., Davis, R.A., 1998. Longshore Sediment Transport Rate in the Surf Zone: Field measurements and Empirical Predictions. Journal of Coastal Research 14 (1). p 269-282.

Wang, P., Smith, R.E., Ebersole, B.A., 2002. Large-Scale Laboratory measurements of Longshore Sediment Transport Under Spilling and Plunging Breakers. Journal of Coastal Research 18 (1). p. 118-135.

Winant, C.D., Inman, D.L., Nordstrom, C.E., 1975. Description of Seasonal beach Changes using Empirical Eigenfunctions. Journal of Geophysical research, 80. .1979-1986.

Wright, L.D., Short, A.D., 1984. Morphodynamics of Beaches and Surf Zones in Australia. CRC Handbook of Coastal processes and Erosion, p. 35-64.